The geochemical role of B-10 enriched boric acid in cemented liquid radioactive wastes

Mojtaba Rostamiparsa[a], István Tolnai[b], Ottó Czömpöly[b], Margit Fábián[b,*], Máté Hegedűs[c], György Falus[a], Csaba Szabó[a,d], Mihály Óvári[b], Csaba Tóbi[b], Péter Kónya[e], Péter Völgyesi[b], Zsuzsanna Szabó-Krausz[a,f]

[a] *Lithosphere Fluid Research Lab, Eötvös Loránd University, Pazmany P. s. 1/C,1117, Budapest, Hungary*

[b] *Centre for Energy Research, Konkoly-Thege Miklós út. 29-33, 1121, Budapest, Hungary*

[c] *Department of Materials Physics, Eötvös Loránd University, Pazmany P. s. 1/C, 1117, Budapest, Hungary*

[d] *Institute of Earth Physics and Space Science, Csatkai E. ut. 6-8, 9400, Sopron, Hungary*

[e] *Directorate of Geology, Supervisory Authority of Regulatory Affairs, Stefania ut. 14, 1143, Budapest, Hungary*

[f] *Centre of Environmental Sciences, Eötvös Loránd University, Pazmany P. s. 1/C, 1117, Budapest, Hungary*

Abstract

Boric acid is a significant radioactive waste generated during the operation of nuclear power plants. Cementitious materials have been widely studied for the immobilization of boric acid. The generally used natural boric acid has been replaced by enriched boric acid for geochemical reasons and are expected to have varied behaviors in cementitious matrices. Results showed that simulated enriched/natural boric acid liquid wastes mostly contain boron in $B(OH)_4^-$ and $B_5O_6(OH)_4^-$ ionic forms, but the mass ratio of these species is higher in enriched boric acid solutions. In function with the concentration of enriched/natural boric acid, the solidified cements show different mineralogy.

Keywords: cement paste; molecular geometry; leaching test; solidified cement

Introduction

Boric acid (BA) solutions, due to the high ability of boron in neutron adsorption, are used widely in nuclear technology [1], [2]. Subsequently, BA waste streams are accounted as the main liquid waste residues from nuclear power plants (NPP) under operation [1]–[7], [8]. These wastes, generally with low to intermediate level of radioactivity, are mostly solidified by different Portland cements enhanced with different mineral and chemical admixtures before subsurface or deep geological deposition [2], [4], [9]–[12]. The application of cement for such aims is due to the satisfying mechanical, radiation and thermal stabilities of cementitious materials, as well as to the potential of hydrated cement phases (e.g., ettringite) to incorporate borates [4], [9], [13]–[16] and calcium silicate hydrate (CSH) to build the radionuclides into their structure [17]–[19]. However, some technical drawbacks of boric acid, such as the corrosive effect inside the operating loops of NPP and the high inherent leachability of boron from final cementitious waste forms had encouraged scientists to find better neutron absorbers [1], [2], [6], [20], [21].

Due to the significant difference between the cross-section of the two boron stable isotopes in thermal neutrons adsorption (σ_{B-10}=3837 barn and σ_{B-11}=0.005 barn) [22], [23], some modern NPPs in Germany, France, Japan, India, and the USA have begun to use ^{10}B enriched boric acid (EBA) up to 90% ^{10}B instead of natural boric acid (NBA), which has 20% ^{10}B abundance [1], [2], [24]. This new EBA neutron absorber can provide a more efficient control system during the reactor operation and also produce significantly less waste volume than the use of NBA (the waste volume drops to 30% when EBA with 60% ^{10}B enrichment is applied) [1], [2], [20],

[25]–[27]. However, despite numerous studies on the technical and economic benefits of EBA during the operation of NPP [20], [26], [28], the waste management aspect of this new promising neutron absorber, especially the compatibility of EBA with cementitious matrices has not received attention previously. Meanwhile, isotopic, elemental, and molecular properties of boron are expected to cause different behaviors of NBA and EBA in cementitious matrices as well as different stability and durability of their final waste forms. The reason is the significant relative mass difference of the ^{10}B and ^{11}B isotopes, and the dependence of borate geometries on pH and boron concentration. The preference of the main borate geometries, which is typically trigonal for the heavier and tetrahedral for the lighter boron isotopes, also contributes to this phenomenon [29]–[38]. The so-called durability of the final waste forms is one of the most important quality parameters of the long-term waste disposals performance assessment analysis [4], [12], [39]–[43].

This study aims to provide better understanding and compare the behavior of NBA and EBA in cementitious structures, as they are the most common hosting matrix for low and intermediate radioactive wastes. The simplest and the most common cement type, ordinary Portland cement (OPC) was used for the experiments. The assessments were focused on leaching tests, in which boron leachability has been selected to be the main parameter to describe the chemical stability of simulated waste forms.

Experimental

For the purposes of this study the following experimental stages were followed: simulation and investigation of NBA- and EBA-liquid radioactive wastes, cementation of the liquid wastes and preparation of solid specimens (simulated final waste forms), mineralogical analysis of solidified cement pastes before leaching, leaching tests, analysis of leachates and, mineralogical analysis of solidified cement pastes after leaching.

Preparation and characterization of simulated liquid boric acid wastes

Simulated wastes with boron concentrations and enrichments specified in Table 1 were prepared at Centre for Energy Research, Hungary. The boron concentration covered a range of 20-60 g/l, which is the average boron concentration of residues in NPP evaporated sludge [3], [4], [20], [44]–[48]. EBA powder (^{10}B>95%) and crystalized ortho-boric acid powder with natural isotopic abundance (^{10}B=19.9%) were used. Both types of boric acid powders were mixed with demineralized (DM) water (conductivity=1.1 μS/cm, pH=7.5 at 23 °C) in the synthesis of the simulated EBA and NBA waste solutions.

Table 1 Specifications of simulated liquid boric acid wastes used for preparing cement pastes.

Sample ID	Boron elemental concentration (g/l)	^{10}B enrichment (%)
LE2 *	20	95
LN2**	20	19.9
LE4	40	95
LN4	40	19.9
LE6	60	95
LN6	60	19.9

*LE: Liquid waste containing EBA

**LN: Liquid waste containing NBA

To increase the boric acid solubility in DM water, having completely homogeneous mixtures, and to decrease the cement retarding effect of boron, the simulated waste solutions were neutralized by adding granular sodium hydroxide with 1.25 of $NaOH/H_3BO_3$ molar ratio. This ratio was an optimum determined by preliminary tests with 0 to 2.5 ratios, which provided the highest alkalinity before the start of any polymerization or crystallization process [4], [6], [21], [34], [49]–[53]. The pH results of this step were benchmarked by geochemical modeling (PHREEQC ver.3, PHREEQC.DAT).

The prepared solutions (Table 1) were analyzed with Raman spectroscopy to clarify the effect of boron isotopic enrichment and concentration on the molecular properties of the simulated liquid wastes. These specifications help understanding the interaction of the solutions with cement clinkers during cement hydration. Raman spectroscopy was carried out on solutions poured into 10 ml volume ceramic sample holder using a HORIBA JobinYvon LabRAM HR 800 Raman micro-spectrometer. A frequency-doubled Nd-YAG green laser with a 532 nm excitation wavelength was used to illuminate the samples, displaying 130 mW at the source and ~50 mW at the sample surface. OLYMPUS 50× (numerical aperture - N.A. = 0.6) and 100× (N.A. = 0.9) objectives were used to focus the laser. A 200 μm confocal hole, 600 grooves/mm optical grating, and 30 s cumulated exposition time were used with 3 accumulations. The spectral resolution of measurements was 3.0 cm^{-1}. Raw spectra were evaluated, including baseline correction and peak fitting using Gaussian-Lorentzian functions with the LabSpec v5.5 software. The contribution of the ceramic sample holder on the Raman spectra was excluded based on blank measurements of the holder with the same acquisition

settings. The measurements were repeated at least five times to reach the uncertainties of the results.

Preparation of simulated waste forms

Cement characterization

Ordinary Portland cement (OPC, CEM I-52,5N), the most common and simplest type of cement, with the given chemical and mineral compositions (Table 2) was mixed with the simulated liquid boric acid wastes (Table 1) and with pure DM water as the reference to prepare cement pastes (Table S1). The applied water-to-cement mass ratio (W/C) was adjusted to 0.4 [4], [12], [21], [39], [40], [49], [54], [55]. The resulting cement pastes have about 2.4-6.8% cement content for the 20-60 g/l boron in liquid wastes, respectively, while the usual mass ratio for the used cement is between 10-12% [20], [21].

Table 2 Chemical and mineralogical specifications of the Portland cement used for preparing the cement pastes. The data is provided by CEMKUT Ltd.

Chemical compositions of major elements									
Oxides	SiO_2	Al_2O_3	Fe_2O_3	CaO	MgO	K_2O	Na_2O	SO_3	Cl^-
(m/m %)	19.71	5.3	3.75	65.03	2.41	0.33	0.43	3.03	0.016
Phase composition									
name	**Alite (C_3S)**	**Belite (C_2S)**	**Tricalcium aluminate (C_3A)**	**Tetracalcium aluminoferrite (C_4AF)**	**Calcium sulfate**				
chemical formula	Ca_3SiO_5	Ca_2SiO_4	$Ca_3Al_2O_6$	$Ca_4Al_2Fe_2O_{10}$	$CaSO_4$				
weight percentage (m/m %)	60.94	10.95	7.7	11.41	5.22				

Mixing, casting and curing

The cement powder was first poured into a mixer (HAUSER DM-601), and then the simulated liquid boric acid waste was added to the cement step by step. The mixture was stirred mechanically (90 rpm for 12 min) at the normal lab conditions (T=23 °C, RH=70%) to obtain a completely homogeneous paste [52]. The wet paste was filled into 2.5 cm diameter and 5 cm height Polyethylene cylindrical molds [56]. The molds were then shaken for 5 minutes to remove air bubbles from the paste [57]. Then, the molds were put in an incubator (VWR-INCU Line 68R) with a fixed temperature of 20±0,1 ºC [56]. The specimens were cured for 28 days, and then they were de-molded by a manual-hydraulic press (SPECAC 25T) [44], [58]

Leaching tests

Leaching tests followed the procedure described in ASTM C1308-21 standard [56]. The cylindrical solid samples with 50 cm^2 contact surface were immersed in 500 ml DM water (leachant), and the resulting solutions (leachates) were changed and sampled in time intervals of 2, 5, 17, and 24 hours and then daily for the next 10 days (Figure S1).

Chemical analysis of the leachates

The pH values of the leachates were measured by calibrated pH meter (Mettler Toledo SevenExcellence). The changes in pH can signify different chemical compounds released into the leachates [39], [40], [59]–[61]. Each leachate was filtered through a cellulose acetate membrane (pore diameter of 0.45 μm) and acidified with ultrapure nitric acid. The solutions were analyzed for the total released boron and its isotopic ratio ($^{10}B/^{11}B$) by inductively coupled plasma optical emission spectrometry (ICP-OES; Perkin Elmer Avio 200) and inductively coupled plasma mass spectrometry (ICP-MS; Thermo Finnigan-Element2), respectively [62].

Chemical and phase analysis of the cementitious specimens

To evaluate the effects of applying different simulated liquid wastes with different concentrations and enrichments and to understand the results of leaching phenomenon on the solidified specimens, morphological, elemental, and mineralogical analyses were carried out on all the cylindrical solid specimens before and after the leaching test. The cylindrical samples were cut in half and after dry polishing of the cut surface (BUEHLER silicon carbide paper; Grit 500) scanning electron microscopy and energy dispersive X-ray spectroscopy (SEM-EDX; Thermo Scientific, Scios 2) measurements were performed. In addition, 3 grams of the exterior rims (affected area) of all the leached and untreated solidified specimens were sampled by a drill, powdered, sieved (63 μm), and analyzed with X-ray diffraction (XRD; Bruker D2 Phaser diffractometer).

Calculation methods

Incremental Fraction Leached (IFL)

Based on the standard procedure, the unitless incremental fraction leached (IFL_n) of boron during the n^{th} test interval is calculated using Eq. 1:

$$IFL_n = a_n^B / A_0^B \quad (1)$$

where a_n^B (mg/l) is the quantity of boron measured in the leachate from the n^{th} test interval, and A_0^B (mg/kg) is the quantity of boron in the solidified specimen at the beginning of the test (Table S1).

Cumulative Fraction Leached (CFL)

The cumulative fraction leached (CFL_j) of boron until the j^{th} interval is calculated by Eq. 2:

$$CFL_j = \sum_{n=1}^{j} a_n^B / A_0^B = \sum_{n=1}^{j} IFL_n \quad (2)$$

Plotting the *CFL* values versus the cumulative time provides a straightforward graphical comparison of leaching data from the various solidified cementitious samples [56]. These results can be later used in modeling calculations to predict the long-term leaching behavior and the overall durability and performance of final waste forms [57].

Results and discussion

Adjustment of pH for the simulated liquid boric acid wastes

The effect of changing the $NaOH/H_3BO_3$ molar ratio on pH of the simulated wastes (both EBA- and NBA-solutions) are shown for experimental and modeling results (Fig. 1). The measured pH curves of EBA and NBA solutions overlap well with each other and with the modeled pH by PHREEQC. Accordingly, there is a generally positive relationship between pH and $NaOH/H_3BO_3$ ratios of 0-1.25, but both methods show no notable pH changes between 1.25-1.5 ratio. On the other hand, during the experiments, the NBA and EBA solutions with $NaOH/H_3BO_3$ ratios above 1.5 got polymerized and crystallized, respectively and became heterogeneous, which should be avoided [53][63]. Therefore, during the preparation of simulated liquid boric acid wastes, the $NaOH/H_3BO_3$ ratio was adjusted to 1.25 to reach the highest possible pH (the longest possible durability for cementitious matrices) but keeping homogeneity [64].

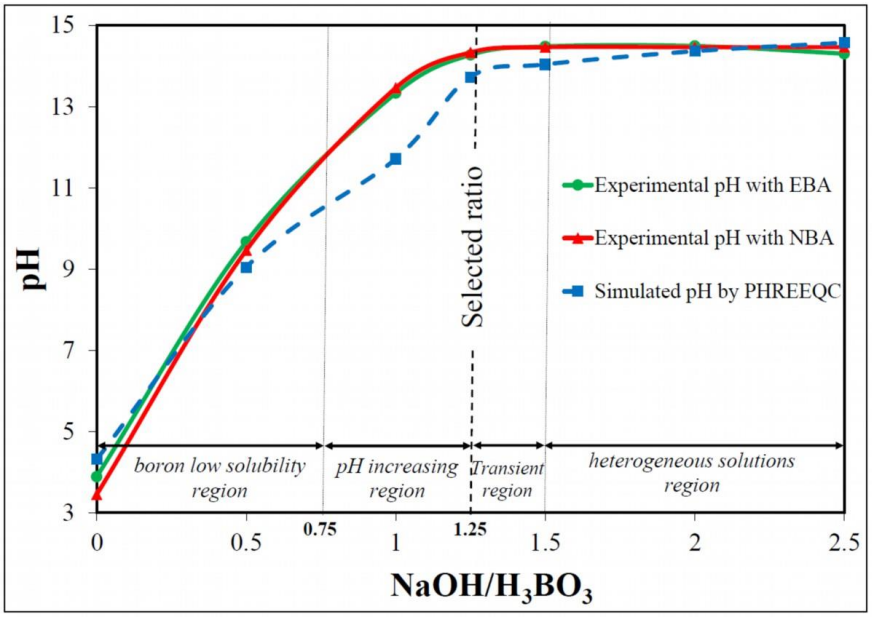

Fig. 1 Measured and modeled effect of changing the $NaOH/H_3BO_3$ ratio on the pH of the simulated liquid boric acid wastes

Results of Raman spectroscopy measurements of simulated liquid wastes

The Raman spectra of the concentrated liquid boric acid wastes (Table 1) are illustrated in Figure 2 for the optimal zone of the characteristic Raman bands of borate solution investigations, 400-1700 cm^{-1} [65]–[71]. For all the samples, four characteristic Raman bands appeared on the spectra (Figure 2). Two bands are at 521 and 745 cm^{-1} which can be identified as for $B_5O_6(OH)_4^-$ and $B(OH)_4^-$ molecules, respectively [65], [66]. The other detected bands are at 1646 cm^{-1} which relates to water [72]–[74]. Bands at 930 cm^{-1} (NBA solutions) or 960 cm^{-1} (EBA solutions) also show up, possibly related to B-O bands in complicated heavy molecules containing boron and sodium atoms [75], [76]. However, their identification is not established yet.

The results of intensity and integrated bands area of the different bands (S_p) are summarised in Table 3.

Table 3 Summary of the Raman spectroscopy analysis on EBA- and NBA-liquid wastes

Band (cm^{-1})	**Intensity** (count)	**S_p±error %** (cm^2)	**$RS_{p(EBA)}$**	**Band** (cm^{-1})	**Intensity** (count)	**S_p±error %** (cm^2)	**$RS_{p(NBA)}$**	**$\Delta RS_{p(EBA/NBA)}$** (%)
LE2				**LN2**				
521.2	599	24798± 3.1	3.8	521	615	32084± 4.7	2.8	26.9

745.8	6037	94899± 0.5		745.8	5592	89809± 0.51		
960.9	265	16930± 2.5		930.7	283	29274± 3.7		
1646.0	765	73206± 3.7		1645.1	835	86118± 3.6		
LE4				**LN4**				
521.2	1397	54810± 2.9	4.2	520.9	675	34088± 4.5	3.6	14.4
746.0	14057	231782± 0.7		745.6	6188	123396± 1.6		
960.1	660	49072± 2.2		930.8	385	45051± 2.9		
1646.8	684	73045± 5.5		1646.5	521	84026± 4.6		
LE6				**LN6**				
521.7	1519	61389± 2.8	4.8	521.7	1027	43996± 3.9	4.6	4.7
745.8	15865	294041± 0.3		745.7	10551	200747± 0.7		
960.0	881	67460± 4.9		930.9	525	48160± 4.1		
1646.7	469	56574± 4.2		1646.9	420	47781± 5.4		

**LE: liquid waste containing 95% ^{10}B enriched boric acid; LN: liquid waste containing natural boric acid; 2, 4, and 6 represent 20, 40, and 60 g/l boron in liquid waste; S_p: integrated area under band; $RS_p = S_{p_{745(B(OH)_4^-)}} / S_{p_{521(B_5O_6(OH)_4^-)}}$; $\Delta RS_{\boldsymbol{p}_{(\boldsymbol{EBA/NBA})}} = (RS_{P_{(EBA)}} - RS_{P_{(NBA)}})/RS_{P_{EBA}} \times 100$ [%]*

For both NBA and EBA solutions, the S_p of the bands at 521, 745, and 930/960 cm^{-1}increase together with boron concentration, whereas the band of water at 1646 cm^{-1}decreases with increasing boron concentration (Figure 2 and Table 3). Additionally, for the known bands of borate molecules at 521 cm^{-1} ($B_5O_6(OH)_4^-$) and 745 cm^{-1} ($B(OH)_4^-$), the ratio of their integrated areas (RS_p, Eq. 3), and the relative comparison of RS_p between NBA and EBA at a fixed concentration ($\Delta RS_{p(EBA/NBA)}$, Eq. 4) are summarised in Table 3. These two provide us the comparability e the molecular ratio of $B_5O_6(OH)_4^-$ and $B(OH)_4^-$ in the studied liquid wastes (Table 3).

$$RS_p = S_{p_{745(B(OH)_4^-)}} / S_{p_{521(B_5O_6(OH)_4^-)}} \quad (3)$$

$$\Delta RS_{p_{(EBA/NBA)}} = (RS_{P_{(EBA)}} - RS_{P_{(NBA)}})/RS_{P_{(EBA)}} \times 100 \quad [\%] \qquad (4)$$

where $S_{p_{745(B(OH)_4^-)}}$ and $S_{p_{521(B_5O_6(OH)_4^-)}}$ are the integrated areas under the specific bands for $B(OH)_4^-$ and $B_5O_6(OH)_4^-$, and $RS_{P_{(EBA)}}$ and $RS_{P_{EBA}}$ are the ratios of the integrated areas of these two bands at EBA and NBA solutions, respectively.

For each boron concentration, the RS_p of the enriched sample ($RS_{P_{(EBA)}}$) is bigger than that of the natural sample ($RS_{P_{(NBA)}}$), and the percentage of this difference ($\Delta RS_{p_{(EBA/NBA)}}$) is decreasing from 26.9 to 4.7% with increasing the boron concentration in the solution from 20 to 60 g/l (Table 3).

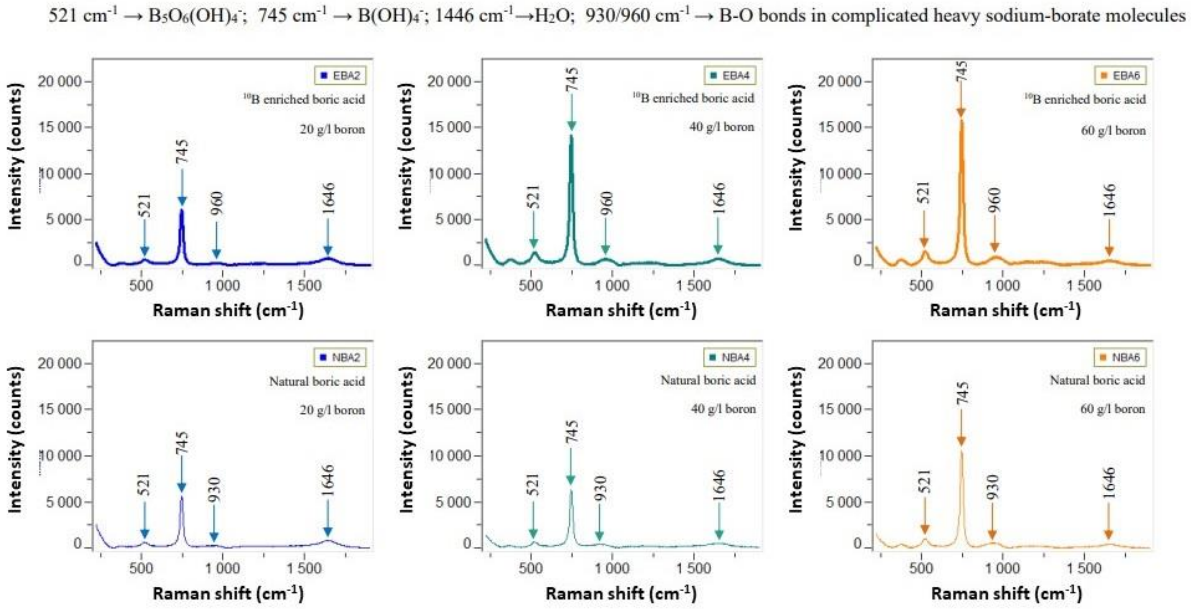

Fig. 2 Raman spectra of the simulated liquid wastes containing different enrichments and concentrations of boric acid. (*NBA: natural boric acid; EBA: ^{10}B enriched boric acid; 2, 4, and 6 represent 20, 40, and 60 g/l boron in the simulated liquid wastes)*

$$S_p RS_p S_{p_{745(B(OH)_4^-)}} S_{p_{521(B_5O_6(OH)_4^-)}} \Delta RS_{\boldsymbol{p_{(EBA/NBA)}}} RS_{P_{(EBA)}} RS_{P_{(NBA)}} RS_{P_{EBA}}$$

Results of XRD analysis of solid samples

The semiquantitative XRD results of all the cementitious solid samples before and after the leaching tests are summarized in Table 4, XRD patterns used for phase identification are presented in Figure S2. For both leached and untreated samples and for both boron enrichments (NBA, 19.9% and EBA, 95% ^{10}B), as the initial concentration of boric acid increases, the hydration level of cement decreases, subsequently the amount of the cement hydration products

(ettringite) significantly increases (Table 4). At each fixed concentration, the solid specimens made with EBA show a higher level of hydration than the specimens made with NBA (Table 4). As the effect of boric acid addition to the cement pastes, the formation of minerals containing boron such as gowerite [CaB_6O_{10}•$5H_2O$] and biringuccite [$Na_2B_5O_8(OH)_2$)•H_2O], were recorded (Table 4).

XRD results also indicate that during the leaching test, all the boron-bearing minerals (i.e., gowerite and biringuccite) have disappeared (dissolved) from the exposed external rim of the NBA specimens, whereas there are some remaining boron-containing phases (biringuccite) at the rim of the specimens made with the highest concentration of EBA (Table 4). Also, a small amount of boron-containing mineral, called meyerhofferite [$Ca_2B_6O_6(OH)_{10}$•$2(H_2O)$] was detected in the specimens before the leaching test that during the experiment have decreased (dissolved) from the exposed external rim of both the NBA and EBA samples (Table 4).

Table 4 Semiquantitative XRD results of the cementitious samples before and after the leaching tests

	Cementitious samples before leaching (m/m %)						
	SE2	SN2	SE4	SN4	SE6	SN6	Ref
Alite	42	50	52	46	58	60	34
Belite	4	11	-	-	-	-	4
Portlandite	26	19	19	18	14	14	39
Ettringite	3	2	-	-	-	-	5
Akermanite	2	1	3	4	4	4	2
Brownmillerite	3	3	2	3	2	3	4
Hydrocalumite	4	3	7	8	7	4	3
Kanemite	-	-	2	6	1	1	-
Biringuccite	8	3	5	6	4	5	-
Gowerite	-	-	1	2	4	4	-
Meyerhofferite	-	-	-	-	-	-	-
Amorph	8	8	9	7	6	5	9
	Cementitious samples after leaching (m/m %)						
	LSE2	LSN2	LSE4	LSN4	LSE6	LSN6	
Alite	50	56	70	72	69	70	
Belite	8	4	-	-	-	-	
Portlandite	22	18	12	10	9	11	
Ettringite	3	2	-	1	-	-	
Akermanite	-	1	1	1	1	1	
Brownmillerite	5	5	4	3	3	2	
Hydrocalumite	4	4	4	4	4	3	
Kanemite	-	-	-	-	-	-	

Biringuccite	-	-	-	-	3	-
Gowerite	-	-	-	-	-	-
Meyerhofferite	-	-	-	-	3	3
Amorph	8	10	9	9	8	10

Ref.: boron concentration is zero in the reference sample; SE: solidified sample with enriched boric acid (95% ^{10}B) before leaching; SN: solidified sample with natural boric acid (19.9% ^{10}B) before leaching; LSE: leached solid sample containing enriched boric acid (95% ^{10}B); LSN: leached solid sample containing natural boric acid (19.8% ^{10}B); Numbers of 2, 4 and 6 represent 20, 40, and 60 g/l boron in the simulated liquid wastes.

Results of SEM analysis of the solidified cement samples

The backscattered-electron (BSE) images of SEM measurements of the solid cement paste samples were analysed before leaching (SE4, SE6, SN4, SN6 and Reference samples) and after leaching (LSE4, LSE6, LSN4 and LSN6) using ImageJ software [77], which is a versatile, open-source used for a variety of tasks, such as simple image enhancements and quantitative image analysis. (Users can perform statistical analysis, extract quantitative data from photographs, and visually explore and edit digital images.) The threshold brightness histogram analysis method algorithm option in the ImageJ software was applied to perform area analysis by highlighting the brightness levels on the surface of the samples to infer and quantify the lighter unhydrated clinker phases from darker hydrated matrix phases (in the Supplementary Materials, Fig S3, which is the original mosaic picture).

The results of the analyses quantified the unhydrated surface areas of the samples before leaching as SE4 (239493.731 μm^2), SE6 (248245.86 μm^2), SN4 (238675.265 μm^2), SN6 (326395.155 μm^2), reference (53714.927 μm^2); whereas samples after leaching as LSE4 (246095.847 μm^2), LSE6 (239826.99 μm^2), LSN4 (316751.896 μm^2) and LSN6 (474797.571 μm^2) using uniform surface area for the statistical analyses. These results seem to indicate a positive correlation between increasing boric acid concentration from 0 g/l in the reference, samples to 60 g/l in SE6 and SN6 showing an increasing surface area of unhydrated clinker phases of 272680.228 μm^2 observed on the samples (Fig. 3) implying the possibility of increased hydration retardation with increasing boric acid concentration. It is also observed from this results that natural boric acid (samples LN4 and LN6) shows a higher retarding on the OPC hydration process than the enriched boric acid (samples SE4 and SE6). The result also indicates that both types of boric acids (either enriched or natural one) show significant hydration retardation effect in comparison with the reference sample (Fig. 3).

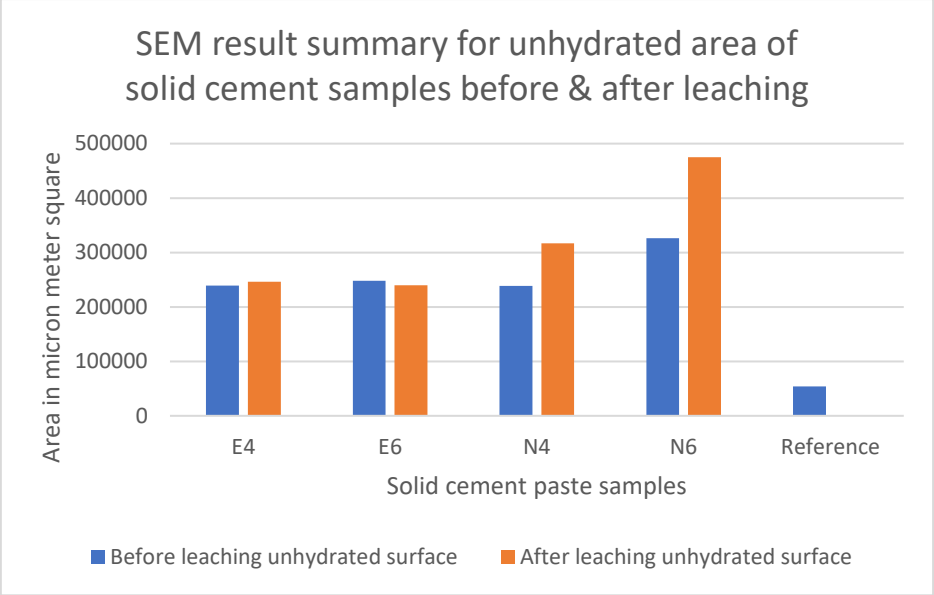

Fig. 3 Summary of SEM analysis of the cementitious specimens before and after the leaching tests using the ImageJ software threshold brightness histogram analysis method algorithm to quantify unhydrated areas: E4 with enriched boric acid of 40 g/l concentration; E6 with enriched boric acid of 60 g/l concentration; N4 natural boric acid of at 40 g/l concentration; N6 natural boric acid of 60 g/l concentration, whereas the reference sample was made with OPC and DM water.

Also, the SEM data are in good agreement with XRD results (Table 4) as boric acid concentration increases so does the amount of unreacted clinker phases observed on the sample surface (Ref. to the original mosaic picture which is supposed to be in Suppl. Mat. as suggested above) and a decrease of the secondary hydration phase production (like ettringite) observed in the XRD results (Table 4). Furthermore, the BSE images show that the leachant (DM water) effect the solidified specimens (compared to the reference sample), and an alteration layer of 300 µm appeared after the leaching period of 11 days (Fig. S4).

Results of leachates analysis

pH measurements

The measured pH for all the leachates shows similar and generally decreasing trends for all the samples (Figure S5). All the pH results are between 11.5-12.3. A notable pH variation ($|\Delta pH| < 0.5$) during the first two days was recorded, which is mostly due to the inequality of the sampling intervals (Figure S5).

Elemental boron release measurements

The concentrations of leached boron (a^B) during each time interval of the leaching test are summarized in Table S2-S4. For all the tests, there was a high peak of boron release at the third interval (17 hours). The results of Table S2-S4 were used to calculate the percentage of leached boron $((\sum^{11\,day} a^B)/A_0)$ from all the solidified specimens (Figure 4). Accordingly, during the leaching period (11 days), the percentage of released boron from all the solidified samples is between 0.62-1.12 m/m %. Furthermore, Figure 4 shows an obvious increase in boron leaching for both EBA and NBA specimens with the growth of the initial boron concentration in the samples. However, at each initial boron concentration, the specimen made with NBA shows a higher percentage of leached boron than that made with EBA (Figure 4).

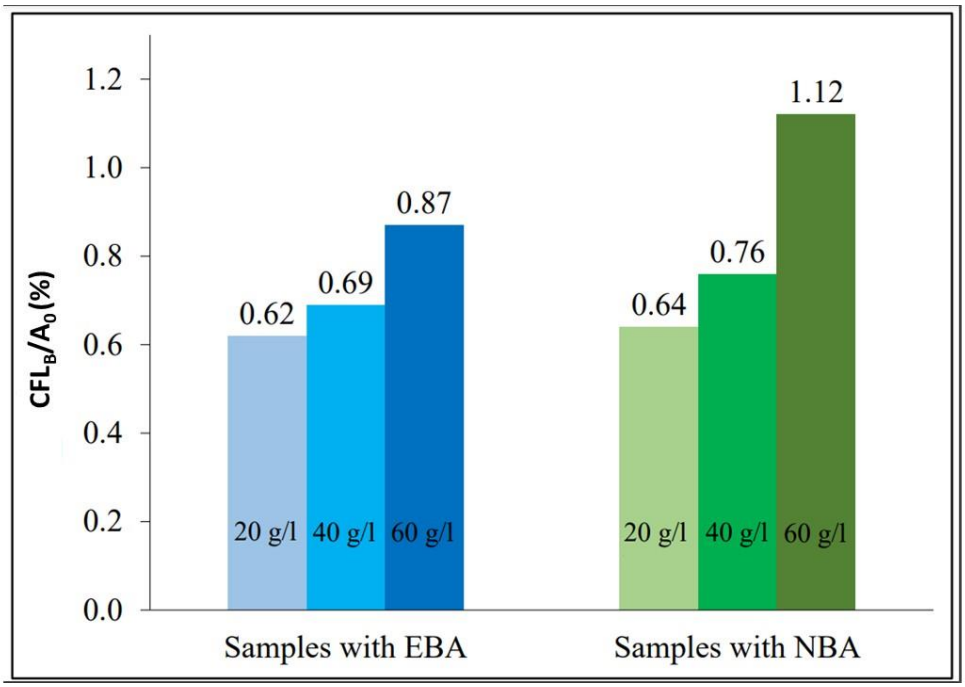

Fig. 4 Percentage of leached boron in contrary to changing boron concentration and enrichment. ($\sum CFL_B$: *cumulative leached boron at the end (11 days) of leaching test; EBA: 95% ^{10}B enriched boric acid; NBA: natural boric acid; A_0= initial boron concentration in the cement pastes)*

The CFL value of boron, calculated using data in Table S2-S4 and following Eqs.1-2, is plotted vs. time in Figure 5. According to these curves, **1)** the *CFL* grows with the initial boron concentration in the samples (20, 40, and 60 g/l boron), and **2)** at each fixed boron concentration, the cementitious specimen made with EBA shows lower *CFL* than that of made with NBA. The differences between EBA and NBA's *CFL* values are getting more significant from 3% up to 29% as the boron concentration in the liquid wastes increases from 20 to 60 g/l.

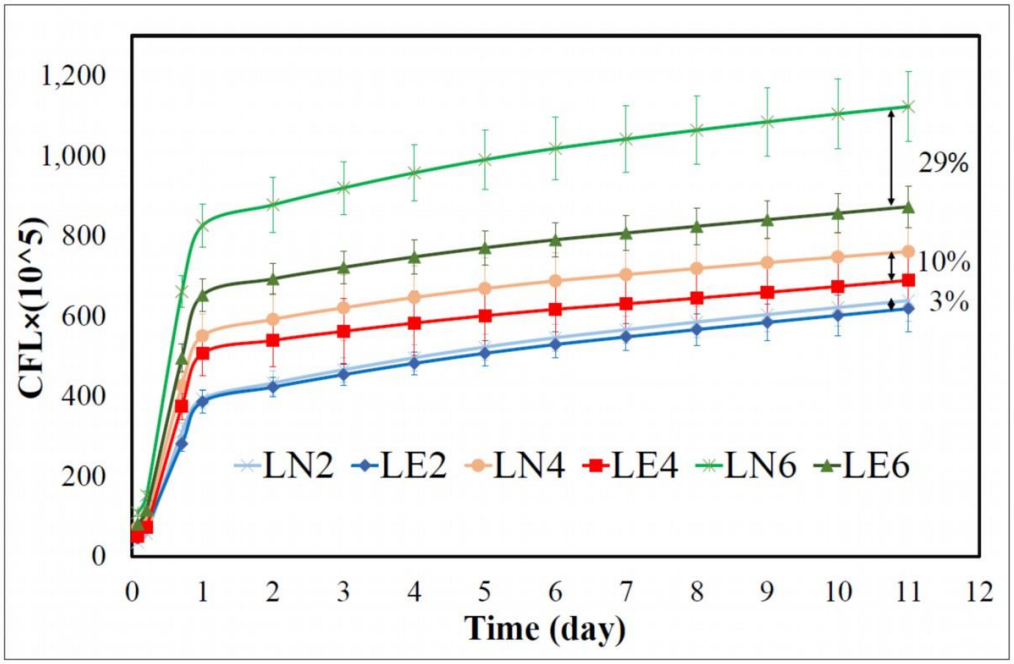

Fig. 5 Cumulative fraction leached (CFL, Eq. 2) of boron vs. time. (*CFL: cumulative fraction of leached boron; LE: leachate from solidified specimens containing 95% ^{10}B enriched boric acid; LN: leachate from solidified specimens containing natural boric acid; 2, 4, and 6 represent 20, 40, and 60 g/l boron in the simulated liquid wastes)*

312

313 In addition, to get a better understanding of boron leaching kinetics, a new parameter, the rate
314 of leaching (R_n), is introduced by Eq. 5, which is a modified formula of Sun et al. [46]:

315

316 $$R_n = \frac{IFL_n}{(D_n \times S/V)} \quad [\text{cm/s}] \qquad (5)$$

317 where R_n is the rate of boron leaching, D_n is the duration of the n^{th} time interval (s), S is the
318 surface area (m^2), and V is the volume of the solidified specimens (m^3). The results of R_n show
319 the net amount of leaching rate independent of the duration of each test interval (Figure 6).

320 As shown in Figure 6, at the beginning of the leaching test (2 hours), all the samples show the
321 highest rate of leaching. This is followed by a short drop in the values (5 hours) and then again,
322 an increase (17 hours). After these changes, all the curves show a continuous decrease in the
323 leaching rate (Figure 6). As a comparison among the cementitious specimens with different
324 boron concentrations and enrichments, the rate of boron leaching (R_n) increased with the initial
325 boron concentration in the samples and is lower for specimens made with EBA than the
326 specimens with NBA (Figures 6). These R_n differences between EBA and NBA specimens are

increased one order of magnitude as the boron concentration in the liquid wastes increases from 20 to 60 g/l.

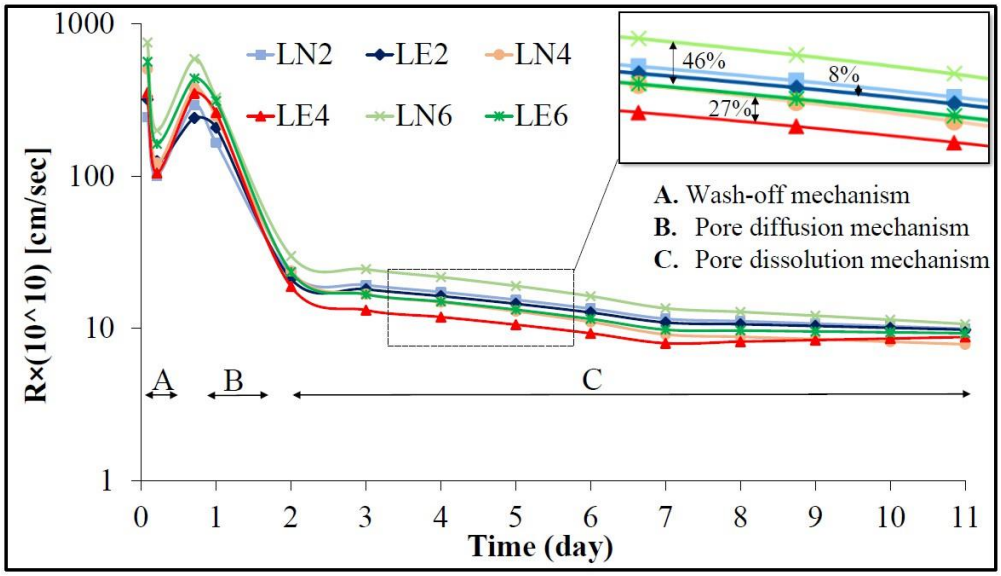

Fig. 6 Logarithmic rate of boron leaching (R_n, Eq. 5) vs. time. (*R: rate of leaching; LE: leachate from solidified specimens containing 95% ^{10}B enriched boric acid; LN: leachate from solidified specimens containing natural boric acid; 2, 4, and 6 represent 20, 40, and 60 g/l boron in the simulated liquid wastes)* [78]

Isotopic distribution of leached boron

The ICP-MS results of boron isotopic distributions in the leachates of EBA and NBA simulated waste forms are plotted in Figures 7 and 8, respectively. For the EBA-specimens the $^{10}B/^{11}B$ ratios in the leachates show a significant decreasing trend during the 11 days of the leaching test (Figure 7). In the beginning of the leaching experiments boron dissolves from the surface and diffuse from the near-surface regim of the samples. The measured ^{10}B abundance (around 90%) is close to the initial one (95%). As the experiment proceeds the boron built-in in the inner part of the sample starts to leach and the ^{10}B abundance decreases suggesting different diffusion coefficient and leachability of the isotopes. [35], [38], [79], [80].

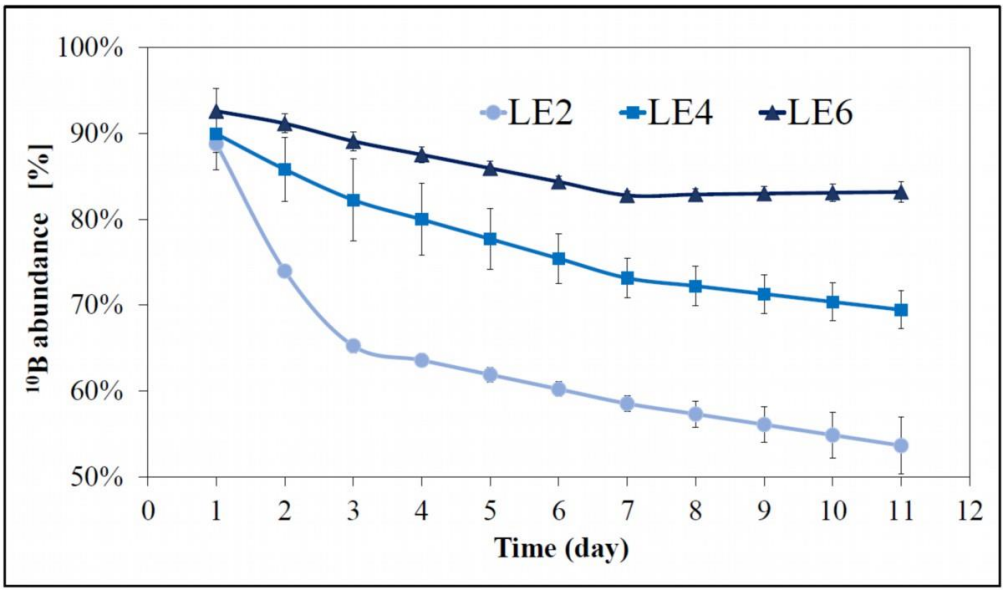

Fig. 7 Isotopic leachability of boron from the solidified specimens containing 95% ^{10}B enriched boric acid (EBA). (*LE: leachate from the specimens containing 95% ^{10}B enriched boric acid; 2, 4, and 6 represent 20, 40, and 60 g/l boron in the simulated liquid wastes.)*

339

340 For the samples from the leaching tests of the NBA-specimens, the ^{10}B/^{11}B ratio showed no
341 significant variation during the test period (Figure 8). The minor changes were lower than the
342 uncertainty of the measurement technique.

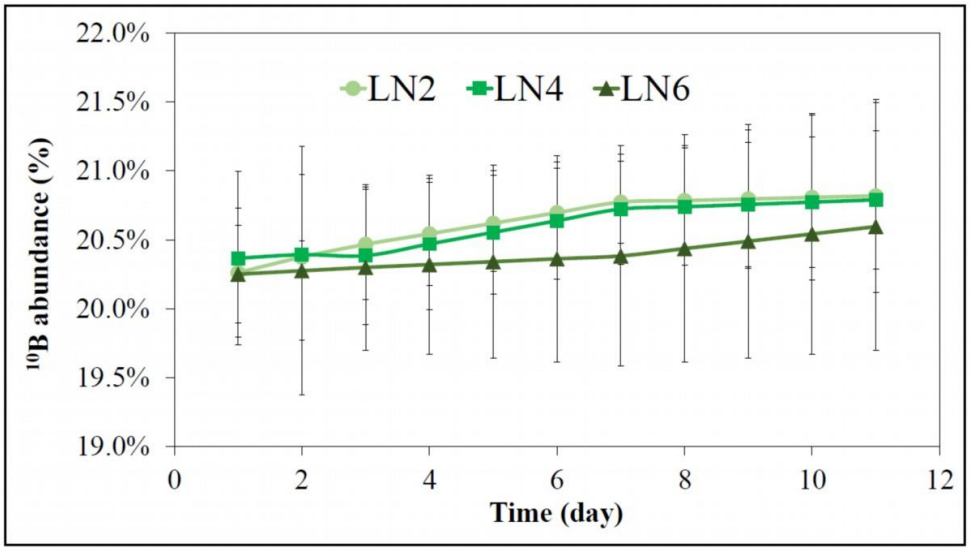

Fig. 8 Isotopic leachability of boron from the solidified specimens containing natural boric acid (NBA). (*LN: leachate from the specimens containing natural boric acid; 2, 4, and 6 represent 20, 40, and 60 g/l boron in the simulated liquid wastes)*

343 **Discussion**

344 **Chemical and geometrical characterizations of EBA- and NBA-liquid wastes**

Since the boron concentration in the studied solutions (20-60 g/l or ~2-6 M boron) is higher than the concentration level where only monoborates are expected (0.2 g/l or 0.025 M boron) [31], [53], [65], [66], [68], [71], [81], [82], all the boron in the studied liquid wastes tends to occur in heavy polyborate molecules ($B_x(OH)_{3x+y}^{y-}$, x>6, and 0<y<3). However, polymerized solutions would create heterogeneous liquid wastes what cannot be effectively immobilized by cementitious materials [83]. To overcome this unfavorable phenomenon (polymerization of the highly concentrated boric acid wastes), the NaOH addition was optimized ($NaOH/H_3BO_3$=1.25, Figure 1), and hence, only moderate-size polyborates ($B_x(OH)_{3x+y}^{y-}$, 3<x<6 and 0<y<3) including $B_3O_3(OH)_4^-$, $B_4O_5(OH)_4^{2-}$, and $B_5O_6(OH)_4^-$ are expected [65], [66]. Meanwhile, the formation possibility of these polyborates is not the same, because at the very high alkalinity (pH>11), the OH^- ions attack the BO_3 bonds in polyborates, depolymerize them and cause to forming $B(OH)_4^-$ ions alternatively [65], [68]. The results of Raman spectroscopy analysis on the studied simulated liquid wastes are in general agreement with previous knowledge from the literature [65]–[68], [82], where, for the simulated liquid wastes, the main significant borate forms are mono tetrahedral borate ($B(OH)_4^-$ with the specific band at 745 cm^{-1}) and poly pentaborate ($B_5O_6(OH)_4^-$ with the specific band at 521 cm^{-1}) (Figure 2).

Furthermore, the results of Raman analysis (Table 3) show that at each boron concentration, the ratio of the integrated area under the main bands (RSp= $S_{B(OH)_4^-}/S_{B_5O_6(OH)_4^-}$) of the EBA solutions is bigger than that of the NBA solution up to 26.9%. This indicates that at each boron concentration, the possibility of $B(OH)_4^-$ formation in the EBA-liquid waste is higher than that of the NBA-liquid waste. This difference is due to the molecular structure and isotopic preference of $B(OH)_4^-$ and $B_5O_6(OH)_4^-$ in EBA and NBA liquid wastes (Figure 9). The molecular structure of $B_5O_6(OH)_4^-$ consists of four trigonal and one tetrahedral borate positions, whereas $B(OH)_4^-$ composed of only one tetrahedral borate position (Figure 9). According to previous knowledge [81], [84]–[87], the trigonal borate geometry is more stable with the heavier boron isotope (^{11}B), whereas the tetrahedral borate geometry prefers the lighter boron isotope (^{10}B). Therefore, resulting in these geometric compositions and isotopic preferences of the borates, the possibility of $B(OH)_4^-$ formation is higher in EBA liquid waste than in NBA liquid waste.

The intensity of the band specific to water (1646 cm^{-1}) decreases with increasing boron concentration (Figure 2 and Table 3). This is due to the decrease in the water-mass ratio in the solutions with increasing the boron concentration from 20 to 60 g/l. cm^{-1}.

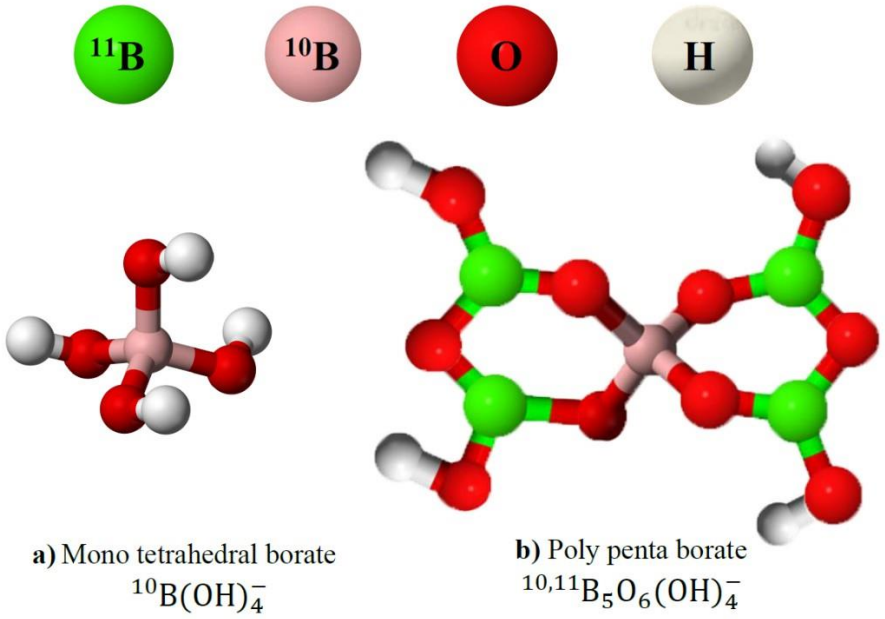

Fig. 9 Molecular structure and isotopic preferences of a) $B(OH)_4^-$ and b) $B_5O_6(OH)_4^-$. $B(OH)_4^-$ consists of one tetrahedral position, which favors ^{10}B and $B_5O_6(OH)_4^-$ consists of one tetrahedral and four trigonal positions, which mostly prefers ^{11}B

375

376 **The solid samples mineralogy vs. the initial boron concentration and enrichment**

377 The influence of changing boric acid concentration on the mineralogy of the cementitious
378 specimens (Table 4 and Figure 3) is mostly related to the boron retarding effect on cement
379 hydration [49], [59], [88]–[90]. The decreasing level of hydration can leave more unreacted
380 clinkers in the cement pastes (Table 4). These remaining clinkers can adversely affect the
381 physical properties of the cement paste, including porosity and compressive strength, and
382 subsequently, the durability of the simulated final waste forms decreases [11], [91]–[93].
383 Furthermore, the formation of ettringite, which has a significant potential for building boron
384 atoms into its structure [4], [9], [13], [14], is detected only in the samples with low boron
385 concentration (Table 4). Therefore, since the increase in boron concentration reduces the
386 cement hydration and also the formation of ettringite, the maximum initial boron concentration
387 in the cementitious matrices (maximum solid loading on cement) should be optimized for both
388 NBA and EBA solidified specimens [20], [21].

The differences in the mineralogy of the solidified specimens with applying NBA or EBA (Table 4) are mostly related to the molecular differences of the simulated liquid boric acid wastes before mixing with cement (section 4.1). Since the liquid wastes containing different types of boric acid enrichments (NBA and EBA) can create varied ratios of the distinct forms and geometries of boron-molecules (Figures 10a and 10c), these molecules can cause different chemical interactions with the cement clinkers and consequently, variable mineralogies can be formed during the cement and liquid wastes mixing (Table 4).

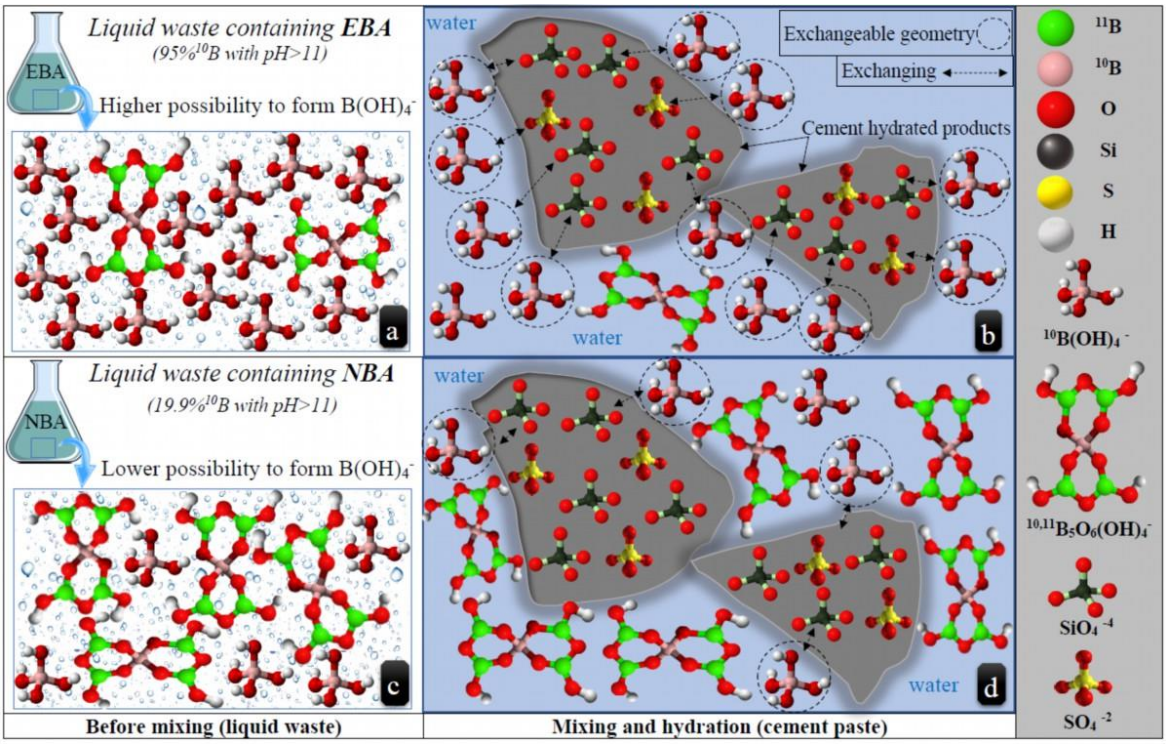

Fig. 10 Two of the most important borate molecule geometries in EBA and NBA solutions and their interaction with cement clinker: a) liquid waste containing 95% ^{10}B enriched boric acid, EBA; b) interaction and substitution of EBA-liquid waste with cement clinker; c) liquid waste containing natural boric acid, NBA; d) interaction and substitution of NBA-liquid waste with cement clinker

Solid samples mineralogy vs. running leaching tests

In accordance with previous studies [42], [61], [94]–[96], the results of our experiments showed that water diffuses from the surface into the interior parts of the cementitious matrices during the leaching test (Figure 3h). Due to the high natural boron-salt solubility [97], all the boron-bearing minerals (i.e., biringuccite and gowerite) get released from the NBA-specimens. However, only some of those minerals from the EBA-specimens are released from the affected depth of the solidified matrix (data of Table 4 for before and after the leaching test), which is

due to the higher stability of borate molecules in EBA solidified specimens as discussed above (section 4.5). During dissolution, the more boron-containing minerals are released from the cementitious structure (NBA-cementitious specimens in this study), the higher porosity becomes, and consequently, shorter durability of the simulated final waste form made with NBA is expected compared with the specimens made with EBA [39], [40].

Boron leachability vs. initial boron concentration

The positive relationship between the total leached boron and the initial boron concentration (Figure 5) is due to the more availability and the subsequent higher possibility of boron-containing minerals getting dissolved from the cementitious host structure [98]. Nevertheless, high leachability can lead to lower chemical stability and durability for the solidified specimens, which is a critical parameter in the long-term disposal of cementitious waste. Not only the net amount of mass (CFL, Figure 5) but also the percentage of total boron leached (Figure 4) shows a continuous growth together with the increase of the initial boron concentration in the specimens. This phenomenon may be related to the porosity increase as the initial boron concentration grows (discussed in section 4.3) and the constraint of cementitious matrices to hold other solid materials or precipitating boron-bearing minerals from boric acid solutions [20], [59], [98].

Boron leachability vs. boron enrichment

At each initial boron concentration, the solidified specimens made with EBA show lower boron leachability (both amount and rate) than those made with NBA (Figures 4-6). This phenomenon is related to the chemical speciation of boric acid introduced in Sections 4.1-4.2 and Figure 10. $^{10}B(OH)_4^-$ [3], [4], [9], [13], [14], [37], [49], [84]. However, in the NBA simulated liquid wastes, the $B(OH)_4^-/B_5O_6(OH)_4^-$ ratio is lower than in the EBA liquid waste (Figure 2 and Table 3). Thus, the more abundant isotope (^{11}B) has lower possibility to locate in the interchangeable tetrahedral borate coordinates of the liquid phase and subsequently has lower possibility of substituting in the above-mentioned sites of the cement paste (Figure 10c-d). The unsubstituted ^{11}B-containing ions and molecules can release from the cementitious matrix effectively when the solidified specimens get contacted with water (Figure 10d). These phenomena are supported by the observations in Figure 7, where after a rapid release of boron from the specimens' surface during the first day (surface wash-off), the abundance of released ^{10}B decreases in time, whereas the total boron leaching increases continuously due to the ^{11}B release [57], [99].

436

437 ## Conclusion

438 This study is the first about the immobilization of the novel radioactive liquid waste containing
439 EBA. The major results and conclusions are the following: a) the simulated radioactive wastes
440 NBA and EBA have different molecular compositions and isotopic specifications, in which pH
441 and boron concentration have the dominant role to constrain these variabilities; b) variation in
442 chemical and isotopic specifications of EBA and NBA solutions causes different interactions
443 between their boron molecules and cement clinker which provide EBA- and NBA-cementitious
444 waste forms with different mineralogies; c) due to the mineralogical modifications, the
445 elemental and isotopic leachabilities of boron from the NBA- and EBA-bearing specimens
446 were different; d) the total amount and the rate of boron leachability from the cementitious
447 specimens containing EBA were lower than that of the specimens containing NBA up to 29%
448 and 46%, respectively; e) these lower values of the amounts and rates of chemical leaching
449 may reflect to a higher long-term stability and durability of EBA simulated waste forms
450 compared to the NBA containing type which should be considered during the long-term
451 disposal design of radioactive wastes; f) this phenomenon can be explained by a combination
452 of unique molecular and isotopic properties of boron in the liquid phase including the high
453 relative mass difference of boron isotopes, the influence of pH and boron concentration on
454 geometry of borates and isotopic preferences of those geometries.

455

456 ## Acknowledgment

457 The authors express their thanks to Levente Illés at *Institute of Technical Physics and Materials*
458 *Science at Centre for Energy Research*, Viktória Gável at *CEMKUT Research & Development*
459 *Ltd.,* Gorkhmaz Abbaszade, László Előd Aradi, Tamas Spránitz, Gabriel Iklaga and others at
460 *Eötvös Loránd University* for their supports during this study.

461 Funding: This work was party supported by the Stipendium Hungaricum Scholarship to
462 Mojtaba Rostamiparsa (FI 80798, 2018-2022); the Premium Postdoctorate Research grant
463 (Premium_2017-13) to Zsuzsanna Szabó-Krausz provided by the Hungarian Academy of
464 Sciences; the ELTE Institutional Excellence Program (1783–3/2018/FEKUTSRAT)
465 to Zsuzsanna Szabó-Krausz and Csaba Szabó funded by the Hungarian Ministry of Human
466 Capacities; and partly supported by the Centre for Energy Research (EK-138/2022) and by the

János Bolyai Research Scholarship to Margit Fábián provided by the Hungarian Academy of Sciences.

Conflict of Interest statement

The authors have no relevant financial or non-financial interests that are relevant to the content of this article. The funding of this work is honestly disclosed in the acknowledgements section.

References

[1] N. Pacey, I. Beadle, A. Heaton, and L. Newsome, “Chemical discharges from nuclear power stations : historic releases and implications for best available techniques (BAT),” Environment Agency, Bristol, 2011.

[2] J. Xu and W. Zhang, “The application of 10B enriched boric acid in nuclear power industry,” *International Conference on Nuclear Engineering, Proceedings, ICONE*, vol. 3, pp. 1–5, 2010, doi: 10.1115/icone18-29042.

[3] A. Palomo and M. Palacios, “Alkali-activated cementitious materials: Alternative matrices for the immobilisation of hazardous wastes - Part I. Stabilisation of boron,” *Cem Concr Res*, vol. 33, no. 2, pp. 281–288, 2003, doi: 10.1016/S0008-8846(02)00963-8.

[4] Q. Sun and J. Wang, “Cementation of radioactive borate liquid waste produced in pressurized water reactors,” *Nuclear Engineering and Design*, vol. 240, no. 10, pp. 3660–3664, 2010, doi: 10.1016/j.nucengdes.2010.07.018.

[5] R. O. Abdel Rahman, D. H. A. Zin El Abidin, and H. Abou-Shady, “Cesium binding and leaching from single and binary contaminant cement-bentonite matrices,” *Chemical Engineering Journal*, vol. 245, pp. 276–287, 2014, doi: 10.1016/j.cej.2014.02.033.

[6] O. Gorbunova, “Cementation of liquid radioactive waste with high content of borate salts,” *J Radioanal Nucl Chem*, vol. 304, no. 1, pp. 361–370, 2015, doi: 10.1007/s10967-014-3886-3.

[7] J. Süssmilch -Lukáš, G.-P. Fabián -Edit, T.-B.-S. Nehme, A. Baranyi, and K. Kopecskó, “Solidification of radioactive evaporator residues with high borate content”, doi: 10.32970/CS.2022.1.4.

[8] A. Baranyi, K. Kopecskó, F. Feil, and L. Gric, “A paksi atomerőmű hulladékainak cementbe ágyazása, és a technológiához tartozó vizsgáló laboratórium kialakítása,” *Vasbetonépítés*, vol. 23, no. 2, pp. 31–40, 2021, doi: 10.32969/vb.2021.2.2.

[9] J. B. Champenois *et al.*, “Crystal structures of Boro-AFm and sBoro-AFt phases,” *Cem Concr Res*, vol. 42, no. 10, pp. 1362–1370, 2012, doi: 10.1016/j.cemconres.2012.06.003.

[10] M. Davraz, H. E. Pehlivanoğlu, S. Kilinçarslan, and I. Akkurt, “Determination of radiation shielding of concrete produced from Portland cement with boron additives,” *Acta Phys Pol A*, vol. 132, no. 3, pp. 702–704, 2017, doi: 10.12693/APhysPolA.132.702.

[11] M. I. Ojovan, G. A. Varlackova, Z. I. Golubeva, and O. N. Burlaka, “Long-term field and laboratory leaching tests of cemented radioactive wastes,” *J Hazard Mater*, vol. 187, no. 1–3, pp. 296–302, 2011, doi: 10.1016/j.jhazmat.2011.01.004.

[12] R. O. Abdel Rahman, R. Ravil Z., R. Nailia R., and O. Michael I., *Cementitious material for nuclear waste immobilization*, First. London - UK: WILEY, 2015. doi: 10.1002/9781118511992.

[13] Y. Hiraga and N. Shigemoto, “Boron uptake behavior during ettringite synthesis in the presence of H3BO3 and in a suspension of ettringite in H3BO3,” *Journal of Chemical Engineering of Japan*, vol. 43, no. 10, pp. 865–871, 2010, doi: 10.1252/jcej.10we160.

[14] X. Xu *et al.*, “Stability and leaching resistance performance of SAC repair and solidification materials exposed to gamma irradiation,” *Constr Build Mater*, vol. 302, no. August, 2021, doi: 10.1016/j.conbuildmat.2021.124309.

[15] H. Poellmann, St. Auer, H.-J. Kuzel, and R. Wenda, “Solid solution of ettringites,” *Cem Concr Res*, vol. 23, no. 2, pp. 422–430, 1993, doi: 10.1016/0008-8846(93)90107-k.

[16] L. J. Csetenyi and F. P. Glasser, Borate Substituted Ettringites. MRS Online Proceedings Library 294, 273–278 (1992). https://doi.org/10.1557/PROC-294-273

[17] E. Duque-Redondo, K. Yamada, I. López-Arbeloa, and H. Manzano, "Cs Retention and Diffusion in C-S-H at Different Ca/Si Ratios," *ChemRxiv*, pp. 1–7, 2018, doi: 10.26434/chemrxiv.6683010.

[18] E. W. Jan Tits, Tomonari Fujita, Messaoud Harfouche, Rainer Dähn, Masaki Tsukamoto, "Radionuclide uptake by calcium silicate hydrates : Case studies with Th (IV) and U (VI) Nuclear Energy and Safety Research Department," Villigen PSI, Switzerland, 2014.

[19] E. Duque-Redondo, K. Yamada, J. S. Dolado, and H. Manzano, "Microscopic mechanism of radionuclide Cs retention in Al containing C-S-H nanopores," *Comput Mater Sci*, vol. 190, no. January, 2021, doi: 10.1016/j.commatsci.2021.110312.

[20] A. Bruggeman *et al.*, *Processing of nuclear power plant waste streams containing boric acid - TECDOC-911*, vol. 28, no. 06. Vienna, Austria: IAEA, 1996.

[21] N. R. Rakhimova, R. Z. Rakhimov, V. P. Morozov, L. I. Potapova, and Y. N. Osin, "Mechanism of solidification of simulated borate liquid wastes with sodium silicate activated slag cements," *J Clean Prod*, vol. 149, pp. 60–69, 2017, doi: 10.1016/j.jclepro.2017.02.066.

[22] S. Mughabghab and D. Garber, "Neutron cross sections, resonance parameters," New York, 1973.

[23] A. Deruytter, G. Debus, K. Lauer, H. Moret, and A. Prosdocimi, "Measurement of the thermal neutron absorption cross section of boron by means of a time of flight technique," Brussels (Belgium), 1962.

[24] A. J. Impink, J. A. Battaglia, and G. G. FasnachtKonopka, John W. Konopka, "Enriched B-10 boric acid control system for a nuclear reactor plant (USA Patent)," 2,561, 1993

[25] Z. Hongwei, Z. Xuehua, and Z. Bao'an, "Synthesis of Enriched 10B Boric Acid of Nuclear Grade," *Transactions of Tianjin University*, vol. 20, no. 1, pp. 458–462, 2014, doi: 10.1007/s12209-014-2303-x.

[26] H. Ocken and K. Garbett, "An Evaluation of Enriched Boric Acid in European PWRs," Electric Power Research Institute. EPRI Report, UK, 2001.

[27] W. Zhang, T. Liu, and J. Xu, "Preparation and characterization of 10B boric acid with high purity for nuclear industry," *Springerplus*, vol. 5, no. 1, 2016, doi: 10.1186/s40064-016-2310-6.

[28] J. Blok, "Update on Use of Enriched Boric Acid in Domestic Pressurized Water Reactors," Electric power research institue; California - USA, 2005.

[29] T. Zhang, D. Li, and L. Meng, "Recent progresses on the boron species in aqueous solution: Structure, phase equilibria, metastable zone width (MZW) and thermodynamic model," *Reviews in Inorganic Chemistry*, vol. 41, no. 1, pp. 49–60, 2021, doi: 10.1515/revic-2020-0012.

[30] H. Ge, Y. Zhou, H. Liu, Y. Fang, and C. Fang, "Molecular interactions in aqueous solutions of polyborates at different acidity based on the Raman spectroscopy data at 25°C," *Russian Journal of Physical Chemistry A*, vol. 91, no. 10, pp. 1925–1931, 2017, doi: 10.1134/S0036024417100119.

[31] T. Hirao, M. Kotaka, and H. Kakihana, "Raman spectra of polyborate ions in aqueous solution," *Journal of Inorganic and Nuclear Chemistry*, vol. 41, no. 8, pp. 1217–1220, 1979.

[32] S. Hameed, H. A. Awad, and R. A. H. Al-Uqaily, "Boron removal from seawater using adsorption and ion exchange techniques," *Ecology, Environment and Conservation*, vol. 26, no. 2, pp. 480–487, 2020.

[33] M. He *et al.*, "Quantification of boron incorporation into synthetic calcite under controlled pH and temperature conditions using a differential solubility technique," *Chem Geol*, vol. 337–338, no. October 2019, pp. 67–74, 2013, doi: 10.1016/j.chemgeo.2012.11.013.

[34] S. Böhlke, C. Schuster, and A. Hurtado, "About the volatility of boron in aqueous solutions of borates with vapour in relevance to BWR-reactors," in *International Conference on the Physics of Reactors " Nuclear power: A sustainable resource,"* Interlaken, Switzerland, 2008, pp. 3089–3096.

[35] H. Kakihana, M. Kotaka, S. Satoh, M. Numura, and M. Okamoto, "Fundamental studies on the Ion exchange separation of boron isotopes," *Bull Chem Soc Jpn*, vol. 50, no. 1, pp. 158–163, 1977, doi: 10.1246/bcsj.50.158.

[36] J. L. Parks and M. Edwards, "Boron in the environment," *Crit Rev Environ Sci Technol*, vol. 35, no. 2, pp. 81–114, 2005, doi: 10.1080/10643380590900200.

[37] K. Kobayashi, Y. Hashimoto, and S. L. Wang, "Boron incorporation into precipitated calcium carbonates affected by aqueous pH and boron concentration," *J Hazard Mater*, vol. 383, no. June 2019, 2020, doi: 10.1016/j.jhazmat.2019.121183.

[38] Y. J. Wang *et al.*, "Mechanism of boron incorporation into calcites and associated isotope fractionation in a steady-state carbonate-seawater system," *Applied Geochemistry*, vol. 98, no. July, pp. 221–236, 2018, doi: 10.1016/j.apgeochem.2018.09.013.

[39] K. Yokozeki, "Leaching from cementitious materials used in radioactive waste disposal sites," in *Thermodynamics, Solubility and Environmental Issues*, T. M. Letcher, Ed., Elsevier B.V., 2007, pp. 169–186. doi: 10.1016/B978-044452707-3/50011-2.

[40] T. Ekström, "Leaching of concrete : experiments and modelling. Division of Building Materials, LTH, Lund University.," 2001.

[41] A. Babaahmadi, "Durability of Cementitious Materials in Long-Term Contact with Water," Chalmers University of Technology - Sweden, 2015.

[42] K. Yokozeki, K. Watanabe, N. Sakata, and N. Otsuki, "Prediction of Changes in Physical Properties due to Leaching of Hydration Products from Concrete," *Journal of Advanced Concrete Technology*, vol. 1, no. 2, pp. 161–171, 2003, doi: 10.3151/jact.1.161.

[43] Z. Zheng, Y. Li, Z. Zhang, and X. Ma, "The impacts of sodium nitrate on hydration and microstructure of Portland cement and the leaching behavior of Sr2+," *J Hazard Mater*, vol. 388, no. September 2019, p. 121805, 2020, doi: 10.1016/j.jhazmat.2019.121805.

[44] E. Hwang and S. Hwang, "Effect of neutralizing agent content on 137-Cs leaching from solidified boric acid waste products," *J Radioanal Nucl Chem*, vol. 148, no. 1, pp. 43–51, 1991, doi: 10.1007/BF02060545.

[45] Q. Sun, J. Li, and J. Wang, "Effect of borate concentration on solidification of radioactive wastes by different cements," *Nuclear Engineering and Design*, vol. 241, no. 10, pp. 4341–4345, 2011, doi: 10.1016/j.nucengdes.2011.08.040.

[46] Q. Sun, J. Li, and J. Wang, "Solidification of borate radioactive resins using sulfoaluminate cement blending with zeolite," *Nuclear Engineering and Design*, vol. 241, no. 12, pp. 5308–5315, 2011, doi: 10.1016/j.nucengdes.2011.08.028.

[47] Hungarian Atomic Energy Authority, "Republic of Hungary, National report, Sixth Report prepared in the framework of the Joint Convention on the Safety of Spent Fuel Management and on the Safety of Radioactive Waste Management," Budapest, 2017.

[48] J. M. Casabonne, "Immobilization of borates and phosphates anions with saturated lime solutions," vol. 59, pp. 133–139, 1993.

[49] Q. Sun, J. Li, and J. Wang, "Effect of borate concentration on solidification of radioactive wastes by different cements," *Nuclear Engineering and Design*, vol. 241, no. 10, pp. 4341–4345, 2011, doi: 10.1016/j.nucengdes.2011.08.040.

[50] C.-T. Huang and W. Yang, "A high volume efficiency process for solidification of boric acid wastes," in *The 4th international topical meeting on "Nuclear thermal hydraulics operations and safety - Taipei - Taiwan*, Taipei - Taiwan, 1994.

[51] L. J. Csetenyi and F. P. Glasser, "Borate retardation of cement set and phase relations in the system Na2O-CaO-B2O3-H2O," *Advances in Cement Research*, vol. 7, no. 25, pp. 13–19, 1995, doi: 10.1680/adcr.1995.7.25.13.

[52] J. B. Champenois *et al.*, "Influence of sodium borate on the early age hydration of calcium sulfoaluminate cement," *Cem Concr Res*, vol. 70, pp. 83–93, 2015, doi: 10.1016/j.cemconres.2014.12.010.

[53] I. Tsuyumoto, T. Oshio, and K. Katayama, "Preparation of highly concentrated aqueous solution of sodium borate," *Inorg Chem Commun*, vol. 10, no. 1, pp. 20–22, 2007, doi: 10.1016/j.inoche.2006.08.019.

[54] H. Lahalle *et al.*, "Influence of the w/c ratio on the hydration process of a magnesium phosphate cement and on its retardation by boric acid," *Cem Concr Res*, vol. 109, pp. 159–174, Jul. 2018, doi: 10.1016/j.cemconres.2018.04.010.

[55] P. C. Aïtcin, "The influence of the water/cement ratio on the sustainability of concrete," in *Lea's Chemistry of Cement and Concrete*, Fifth.Elsevier Ltd, 2019, pp. 807–826. doi: 10.1016/B978-0-08-100773-0.00017-4.

[56] "ASTM C1308-21, Standard Test Method for Accelerated Leach Test for Diffusive Releases from Solidified Waste." ASTM International, West Conshohocken, PA, 2021. doi: 10.1520/C1308-21.

[57] R. O. Abdel Rahman, A. A. Zaki, and A. M. El-Kamash, "Modeling the long-term leaching behavior of 137Cs, 60Co, and 152,154Eu radionuclides from cement-clay matrices," *J Hazard Mater*, vol. 145, no. 3, pp. 372–380, 2007, doi: 10.1016/j.jhazmat.2006.11.030.

[58] A. E. Osmanlioglu, "Immobilization of radioactive waste by cementation with purified kaolin clay," *Waste Management*, vol. 22, no. 5, pp. 481–483, 2002.

[59] M. Davraz, "The effect of boron compound to cement hydration and controllability of this effect," *Acta Phys Pol A*, vol. 128, no. 2, pp. 26–33, 2015, doi: 10.12693/APhysPolA.128.B-26.

[60] L. Boulard and R. Kautenburger, "Short-term elemental release from Portland cement concrete in hypersaline leaching conditions," *Advances in Cement Research*, vol. 32, no. 4, pp. 148–157, 2020, doi: 10.1680/jadcr.18.00085.

[61] K. Yokozeki, K. Watanabe, N. Sakata, and N. Otsuki, "Modeling of leaching from cementitious materials used in underground environment," *Appl Clay Sci*, vol. 26, no. 1-4 SPEC. ISS., pp. 293–308, 2004, doi: 10.1016/j.clay.2003.12.027.

[62] W. Zhang, Y. Tang, and J. Xu, "Online determination of boron isotope ratio in boron trifluoride by infrared spectroscopy," *Applied Sciences (Switzerland)*, vol. 8, no. 12, pp. 1–10, 2018, doi: 10.3390/app8122509.

[63] Y. Zhou, C. Fang, Y. Fang, and F. Zhu, "Polyborates in aqueous borate solution: A Raman and DFT theory investigation," *Spectrochim Acta A Mol Biomol Spectrosc*, vol. 83, no. 1, pp. 82–87, Dec. 2011, doi: 10.1016/j.saa.2011.07.081.

[64] E. Revetegat, C. Richet, and P. Gegout, "EFFECT OF pH ON THE DURABILITY OF CEMENT PASTES," *Cement and concrete*, vol. 22, pp. 259–272, 1992, doi: 10.1016/0008-8846(92)90064-3.

[65] Y. Zhou, C. Fang, Y. Fang, and F. Zhu, "Polyborates in aqueous borate solution: A Raman and DFT theory investigation," *Spectrochim Acta A Mol Biomol Spectrosc*, vol. 83, no. 1, pp. 82–87, 2011, doi: 10.1016/j.saa.2011.07.081.

[66] L. M. S. G. A. Applegarth, C. C. Pye, J. S. Cox, and P. R. Tremaine, "Raman Spectroscopic and ab Initio Investigation of Aqueous Boric Acid, Borate, and Polyborate Speciation from 25 to 80 °c," *Ind Eng Chem Res*, vol. 56, no. 47, pp. 13983–13996, 2017, doi: 10.1021/acs.iecr.7b03316.

[67] H. Ge, Y. Zhou, H. Liu, Y. Fang, and C. Fang, “Molecular interactions in aqueous solutions of polyborates at different acidity based on the Raman spectroscopy data at 25°C,” *Russian Journal of Physical Chemistry A*, vol. 91, no. 10, pp. 1925–1931, 2017, doi: 10.1134/S0036024417100119.

[68] Y. Q. Zhou, C. H. Fang, Y. Fang, F. Y. Zhu, and L. D. Cao, “Polyborates in aqueous sodium borate solution at 298.15 K,” *Asian Journal of Chemistry*, vol. 24, no. 1, pp. 29–32, 2012.

[69] R. Thomas, “Determination of the H3BO3 concentration in fluid and melt inclusions in granite pegmatites by laser Raman microprobe spectroscopy,” *American Mineralogist*, vol. 87, no. 1, pp. 56–68, 2002, doi: 10.2138/am-2002-0107.

[70] J. E. Spessard, “INVESTIGATIONS OF BORATE EQUILIBRIA IN N E U T R A L SALT SOLUTIONS THE IONIC medium method has been used to investigate borate equilibria in aqueous salt solutions [I-5]. The entire titration curve of boric acid was fitted borates in solution was found,” vol. 32, no. 1957, 1970.

[71] A. M. Duffin, C. P. Schwartz, A. H. England, J. S. Uejio, D. Prendergast, and R. J. Saykally, “PH-dependent x-ray absorption spectra of aqueous boron oxides,” *Journal of Chemical Physics*, vol. 134, no. 15, 2011, doi: 10.1063/1.3574838.

[72] Z. Du, J. Chen, W. Ye, J. Guo, X. Zhang, and R. Zheng, “Investigation of two novel approaches for detection of sulfate ion and methane dissolved in sediment pore water using Raman spectroscopy,” *Sensors (Switzerland)*, vol. 15, no. 6, pp. 12377–12388, 2015, doi: 10.3390/s150612377.

[73] W. M. Vibrations and R. Spectroscopy, “PhysicsOpenLab Water Molecule Vibrations with Raman Spectroscopy,” pp. 1–10, 2022.

[74] “Spectral Search | PublicSpectra.” https://publicspectra.com/SpectralSearch (accessed Aug. 06, 2022).

[75] T. Furukawa and W. B. White, “Raman spectroscopic investigation of sodium borosilicate glass structure,” *J Mater Sci*, vol. 16, no. 10, pp. 2689–2700, 1981, doi: 10.1007/bf00552951.

[76] J. Gharavi-Naeini, K. W. Yoo, and N. A. Stump, “Characterization of Barium Borate Frameworks Using Raman Spectroscopy,” *Appl Spectrosc*, vol. 72, no. 4, pp. 627–633, 2018, doi: 10.1177/0003702817748952.

[77] M.D. Abramoff, P.J. Magalhaes and S.J. Ram, "Image Processing with ImageJ". Biophotonics International, volume 11, issue 7, pp. 36-42, 2004.

[78] R. ABDELRAHMAN, A. ZAKI, and A. ELKAMASH, “Modeling the long-term leaching behavior of 137Cs, 60Co, and 152,154Eu radionuclides from cement–clay matrices,” *J Hazard Mater*, vol. 145, no. 3, pp. 372–380, Jul. 2007, doi: 10.1016/j.jhazmat.2006.11.030.

[79] K. Klochko, A. J. Kaufman, W. Yao, R. H. Byrne, and J. A. Tossell, “Experimental measurement of boron isotope fractionation in seawater,” *Earth Planet Sci Lett*, vol. 248, no. 1–2, pp. 276–285, 2006, doi: 10.1016/j.epsl.2006.05.034.

[80] W. Kloppmann, E. Petelet-Giraud, C. Guerrot, L. Cary, and H. Pauwels, “Extreme Boron Isotope Ratios in Groundwater,” *Procedia Earth and Planetary Science*, vol. 13, no. 1, pp. 296–300, 2015, doi: 10.1016/j.proeps.2015.07.069.

[81] Y. Liu and J. A. Tossell, “Ab initio molecular orbital calculations for boron isotope fractionations on boric acids and borates,” *Geochim Cosmochim Acta*, vol. 69, no. 16, pp. 3995–4006, 2005, doi: 10.1016/j.gca.2005.04.009.

[82] R. E. Mesmer, C. F. Baes, and F. H. Sweeton, “Acidity measurments at elevated temperatures,” *Inorg Chem*, vol. 11, pp. 537–543, 1972.

[83] J.-B. Champenois *et al.*, “Influence of sodium borate on the early age hydration of calcium sulfoaluminate cement,” *Cem Concr Res*, vol. 70, pp. 83–93, Apr. 2015, doi: 10.1016/j.cemconres.2014.12.010.

[84] H. Marschall and G. Foster, *Advances in Isotope Geochemistry- Boron isotopes*. Switzerland: Springer, 2018. doi: 10.1007/978-3-319-64666-4.

[85] T. Chen, J. Lyu, Q. Wang, P. Bai, Y. Wu, and X. Guo, "Mechanistic study on boron adsorption and isotopic separation with magnetic magnetite nanoparticles," *Materials Science*, vol. 56, pp. 4624–4640, 2021, doi: 10.1007/s10853-020-05546-x.

[86] Y.-J. Wang *et al.*, "Mechanism of boron incorporation into calcites and associated isotope fractionation in a steady-state carbonate-seawater system," *Applied Geochemistry*, vol. 98, no. September, pp. 221–236, Nov. 2018, doi: 10.1016/j.apgeochem.2018.09.013.

[87] "Boron stable isotopes," in *Encyclopedia of Geochemistry*, Springer International Publishing AG, 2016. doi: 10.1007/978-3-319-39193-9.

[88] M. Davraz, "The effects of boron compounds on the properties of cementitious composites," *Science and Engineering of Composite Materials*, vol. 17, no. 1, pp. 1–17, 2010, doi: 10.1515/secm.2010.17.1.1.

[89] V. M. Vieira and C. C. Oliveira de Tello, "Study of Chemical Additives in the Cementation of Radioactive Waste of PWR Reactors," *Universal Journal of Chemistry*, vol. 4, no. 1, pp. 1–9, 2016, doi: 10.13189/ujc.2016.040101.

[90] R. J. van Eijk and H. J. H. Brouwers, "Modelling the effects of waste components on cement hydration," *Waste Management Series*, vol. 1, no. C, pp. 685–694, 2000, doi: 10.1016/S0713-2743(00)80078-1.

[91] M. Davraz, "The effects of boron compounds on the properties of cementitious composites," *Science and Engineering of Composite Materials*, vol. 17, no. 1, pp. 1–17, 2010, doi: 10.1515/secm.2010.17.1.1.

[92] M. I. Ojovan and W. E. Lee, "Immobilisation of Radioactive Waste in Cement," in *An Introduction to Nuclear Waste Immobilisation*, Elsevier B.V., 2014, pp. 205–232. doi: 10.1016/b978-0-08-099392-8.00015-2.

[93] S. E. Hosam El-Din Saleh, Talat Bayoumi, "Characterizations of Polyester-Cement Composites Used for the Immobilization of Radioactive Wastes," in *Polyester*, H. M. Saleh, Ed., IntechOpen, 2012, pp. 257–290. doi: 10.5772/2748.

[94] S. Kamali, M. Moranville, and S. Leclercq, "Material and environmental parameter effects on the leaching of cement pastes: Experiments and modelling," *Cem Concr Res*, vol. 38, no. 4, pp. 575–585, 2008, doi: 10.1016/j.cemconres.2007.10.009.

[95] S. P. Zhang and L. Zong, "Evaluation of relationship between water absorption and durability of concrete materials," *Advances in Materials Science and Engineering*, vol. 2014, 2014, doi: 10.1155/2014/650373.

[96] P. Faucon *et al.*, "Leaching of cement: Study of the surface layer," *Cem Concr Res*, vol. 26, no. 11, pp. 1707–1715, 1996, doi: 10.1016/S0008-8846(96)00157-3.

[97] V. Kochkodan, N. Bin Darwish, and Nidal Hilal, "The Chemistry of Boron in Water," in *Boron Separation Processes*, 1st editio.Swansea University: Elsevier, 2015, pp. 35–63. doi: 10.1016/B978-0-444-63454-2.00002-2.

[98] H. M. Saleh and H. A. Shatta, "Immobilization of Simulated Borate Radioactive Waste Solution in Cement-Poly(methylmethacrylate) Composite: Mechanical and Chemical Characterizations," *Journal of Nuclear Chemistry*, vol. 2013, pp. 1–7, 2013, doi: 10.1155/2013/749505.

[99] W. Zhang and J. Wang, "Leaching performance of uranium from the cement solidified matrices containing spent radioactive organic solvent," *Ann Nucl Energy*, vol. 101, pp. 31–35, Mar. 2017, doi: 10.1016/j.anucene.2016.09.055.

735

Supplementary information

Table S1 Specification of the simulated waste forms

Sample ID	Initial boron concentration in cement past, A_0 (ppm)	^{10}B enrichment (%)
Ref*	0	-
SE2	5714	95
SN2	5714	19.9
SE4	11428	95
SN4	11428	19.9
SE6	17142	95
SN6	17142	19.9

Ref*: Reference sample without boron content

SE: Solidified cement paste containing enriched boric acid (95% ^{10}B)

SN: Solidified cement paste containing natural boric acid (19.9% ^{10}B)

Table S2 The concentrations of leached boron (a^B) during the time interval of the leaching test in case of 20 g/l boron is modelled liquid waste.

	Samples made with EBA		Samples made with NBA	
	a^B(ppm)	Σa^B (ppm)	a^B(ppm)	Σa^B (ppm)
Time intervals	Boron in liquid waste = 20 g/l and in cement paste A_0 = 5714 ppm			
2 hr (0.083 day)	2.6 ± 0.1	2.63	2.01 ± 0.01	2.01
5 hr (0.21 day)	1.5 ± 0.1	4.17	1.24 ± 0.02	3.25
17 hr (0.71 day)	11.9 ± 0.2	16.08	14.5 ± 0.3	17.72
1st day	5.9 ± 0.1	22.07	4.76 ± 0.04	22.48
2nd day	2.09 ± 0.01	24.16	2.26 ± 0.05	24.74
3rd day	1.78 ± 0.01	25.94	1.90 ± 0.03	26.64
4th day	1.61 ± 0.01	27.55	1.71 ± 0.02	28.35
5th day	1.43 ± 0.02	28.98	1.52 ± 0.02	29.87
6th day	1.25 ± 0.01	30.24	1.33 ± 0.02	31.20
7th day	1.08 ± 0.01	31.31	1.14 ± 0.01	32.34
8th day	1.05 ± 0.02	32.37	1.10 ± 0.02	33.44
9th day	1.02 ± 0.03	33.39	1.06 ± 0.02	34.50
10th day	0.99 ± 0.04	34.38	1.02 ± 0.03	35.52
11th day	0.97 ± 0.04	35.35	0.98 ± 0.03	36.50

*a^B: realeased boron; Σa^B: cumulative released boron; EBA: enriched boric acid (95% ^{10}B); NBA: natural boric acid (19.9% ^{10}B); A_0: initial boron concentration in the solidified cement pastes; with 20 g/l boron in the liquid wastes

749 **Tables S3** The concentrations of leached boron (a^B) during the time interval of the leaching
750 test in case of 40 g/l boron is modelled liquid waste.

	Samples made with EBA		Samples made with NBA	
	a^B(ppm)	Σa^B (ppm)	a^B(ppm)	Σa^B (ppm)
Time intervals	Boron in liquid waste = 40 g/l and in cement paste A_0 = 11428 ppm			
2 hr (0.083 day)	5.8 ± 0.4	5.83	8.3 ± 0.2	8.30
5 hr (0.21 day)	2.59 ± 0.03	8.42	3.0 ± 0.1	11.31
17 hr (0.71 day)	34 ± 1	42.87	37.4 ± 0.3	48.75
1st day	15.1 ± 0.9	57.92	14.2 ± 0.5	62.93
2nd day	3.7 ± 0.3	61.64	4.71 ± 0.03	67.64
3rd day	2.6 ± 0.2	64.24	3.3 ± 0.1	70.95
4th day	2.3 ± 0.2	66.58	2.9 ± 0.1	73.88
5th day	2.1 ±0.2	68.67	2.6 ± 0.1	76.44
6th day	1.8 ± 0.1	70.50	2.18 ± 0.04	78.62
7th day	1.6 ± 0.1	72.08	1.80 ± 0.04	80.42
8th day	1.6 ± 0.1	73.69	1.74 ± 0.04	82.15
9th day	1.7 ± 0.1	75.34	1.68 ± 0.04	83.83
10th day	1.7 ± 0.1	77.04	1.61 ± 0.04	85.44
11th day	1.7 ± 0.1	78.77	1.55 ± 0.04	86.99

751 $^*a^B$: realeased boron; Σa^B: cumulative released boron; EBA: enriched boric acid (95% ^{10}B);
752 NBA: natural boric acid (19.9% ^{10}B); A_0: initial boron concentration in the solidified cement
753 pastes; with 40 g/l boron in the liquid wastes

754

755 **Table S4** The concentrations of leached boron (a^B) during the time interval of the leaching test
756 in case of 60 g/l boron is modelled liquid waste.

	Samples made with EBA		Samples made with NBA	
	a^B(ppm)	Σa^B (ppm)	a^B(ppm)	Σa^B (ppm)
Time intervals	Boron in liquid waste = 60 g/l and in cement paste A_0 = 17142 ppm			
2 hr (0.083 day)	13.9 ± 0.1	13.92	18.7 ± 0.4	18.66
5 hr (0.21 day)	6.03 ± 0.02	19.95	7.4 ± 0.2	26.05
17 hr (0.71 day)	65 ± 1	84.90	87 ± 1	113.29
1st day	27.0 ± 0.3	111.85	28.4 ± 0.4	141.64
2nd day	6.95 ± 0.04	118.80	8.9 ± 0.3	150.50
3rd day	4.95 ± 0.03	123.75	7.2 ± 0.2	157.74
4th day	4.44 ± 0.03	128.19	6.4 ± 0.1	164.17
5th day	3.93 ± 0.03	132.12	5.6 ± 0.1	169.80
6th day	3.41 ± 0.02	135.53	4.8 ± 0.1	174.62
7th day	2.90 ± 0.01	138.43	4.0 ± 0.1	178.63
8th day	2.86 ± 0.01	141.29	3.8 ± 0.1	182.42
9th day	2.83 ± 0.02	144.12	3.6 ± 0.1	186.01
10th day	2.79 ± 0.02	146.90	3.4 ± 0.1	189.38

11th day	2.75 ± 0.02	149.66	3.2 ± 0.1	192.54

757 $^{*}a^{B}$: realeased boron; Σa^{B}: cumulative released boron; EBA: enriched boric acid (95% ^{10}B);
758 NBA: natural boric acid (19.9% ^{10}B); A_0: initial boron concentration in the solidified cement
759 pastes; with 60 g/l boron in the liquid wastes

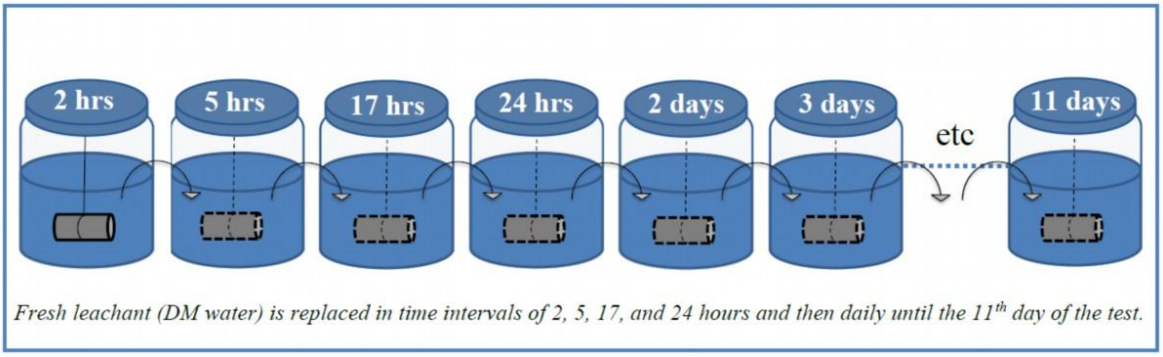

Fig. S1 Schematic diagram of ASTM C1308-21 leaching protocol.

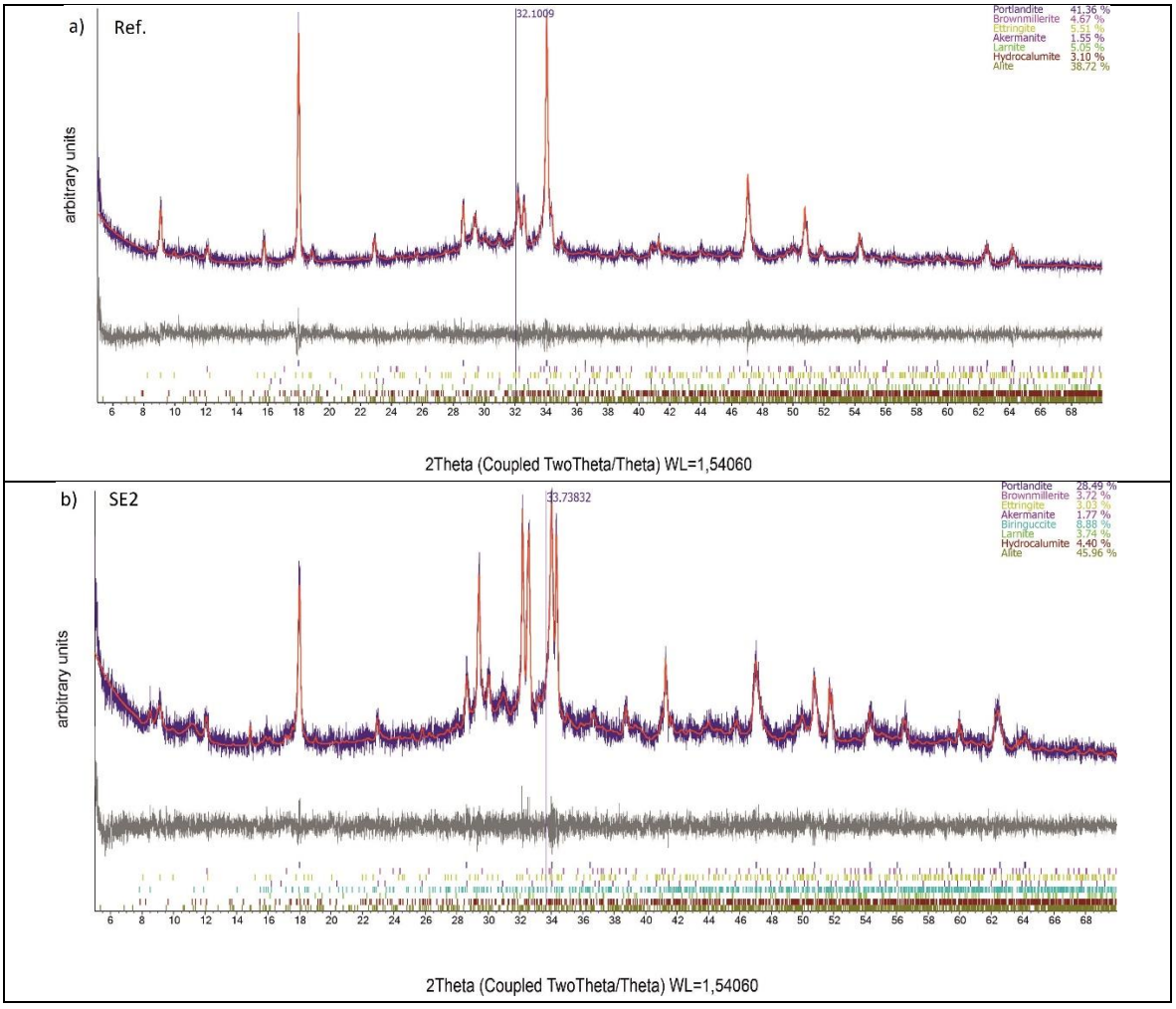

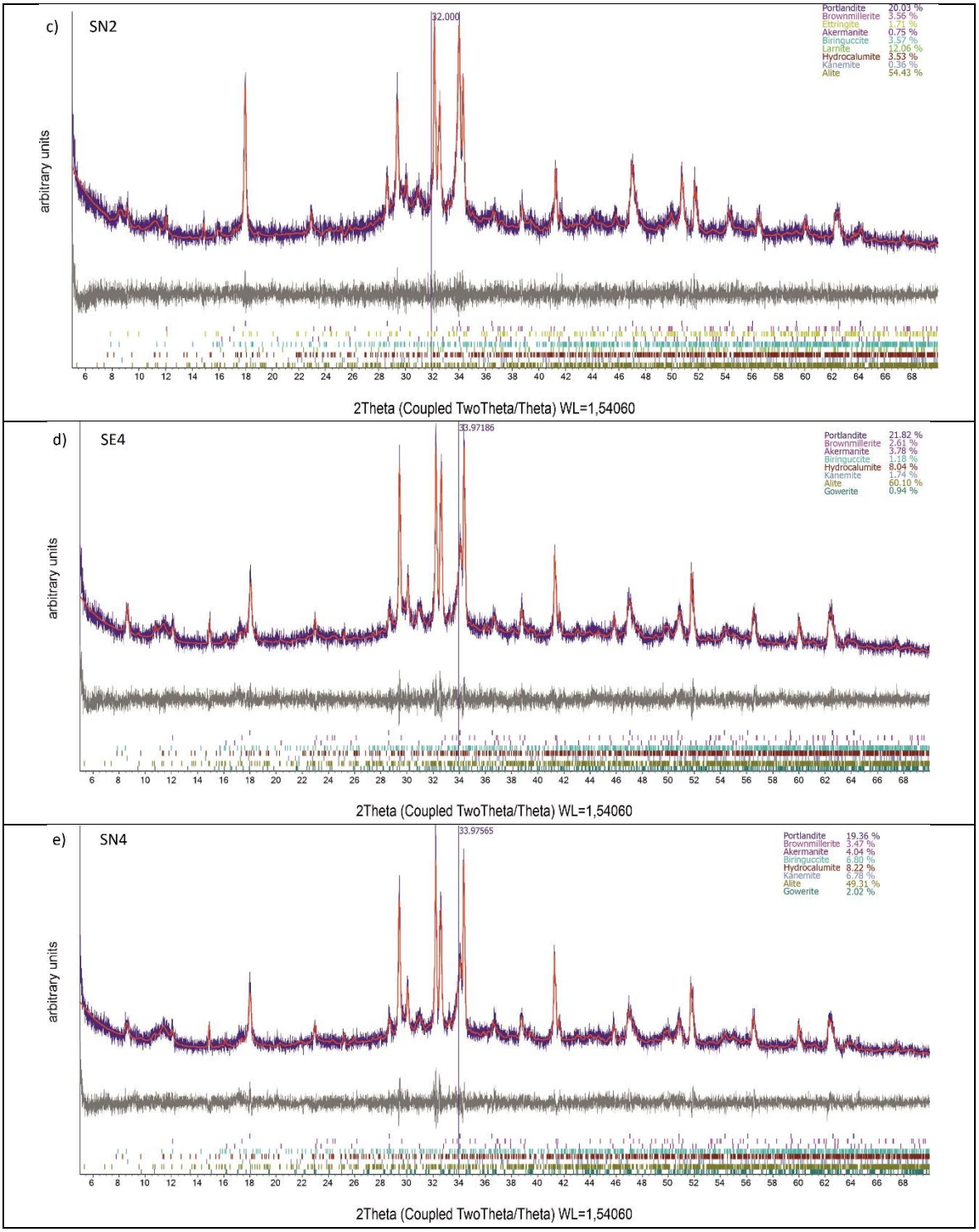
c)
SN2
32.000
Portlandite 20.03 %
Brownmillerite 3.56 %
Ettringite 1.71 %
Akermanite 0.75 %
Biringuccite 3.57 %
Larnite 12.06 %
Hydrocalumite 3.53 %
Kanemite 0.36 %
Alite 54.43 %
arbitrary units
2Theta (Coupled TwoTheta/Theta) WL=1,54060
d)
SE4
33.97186
Portlandite 21.82 %
Brownmillerite 2.61 %
Akermanite 3.78 %
Biringuccite 1.18 %
Hydrocalumite 8.04 %
Kanemite 1.74 %
Alite 60.10 %
Goweríte 0.94 %
arbitrary units
2Theta (Coupled TwoTheta/Theta) WL=1,54060
e)
SN4
33.97565
Portlandite 19.36 %
Brownmillerite 3.47 %
Akermanite 4.04 %
Biringuccite 6.80 %
Hydrocalumite 8.22 %
Kanemite 6.78 %
Alite 49.31 %
Goweríte 2.02 %
arbitrary units
2Theta (Coupled TwoTheta/Theta) WL=1,54060

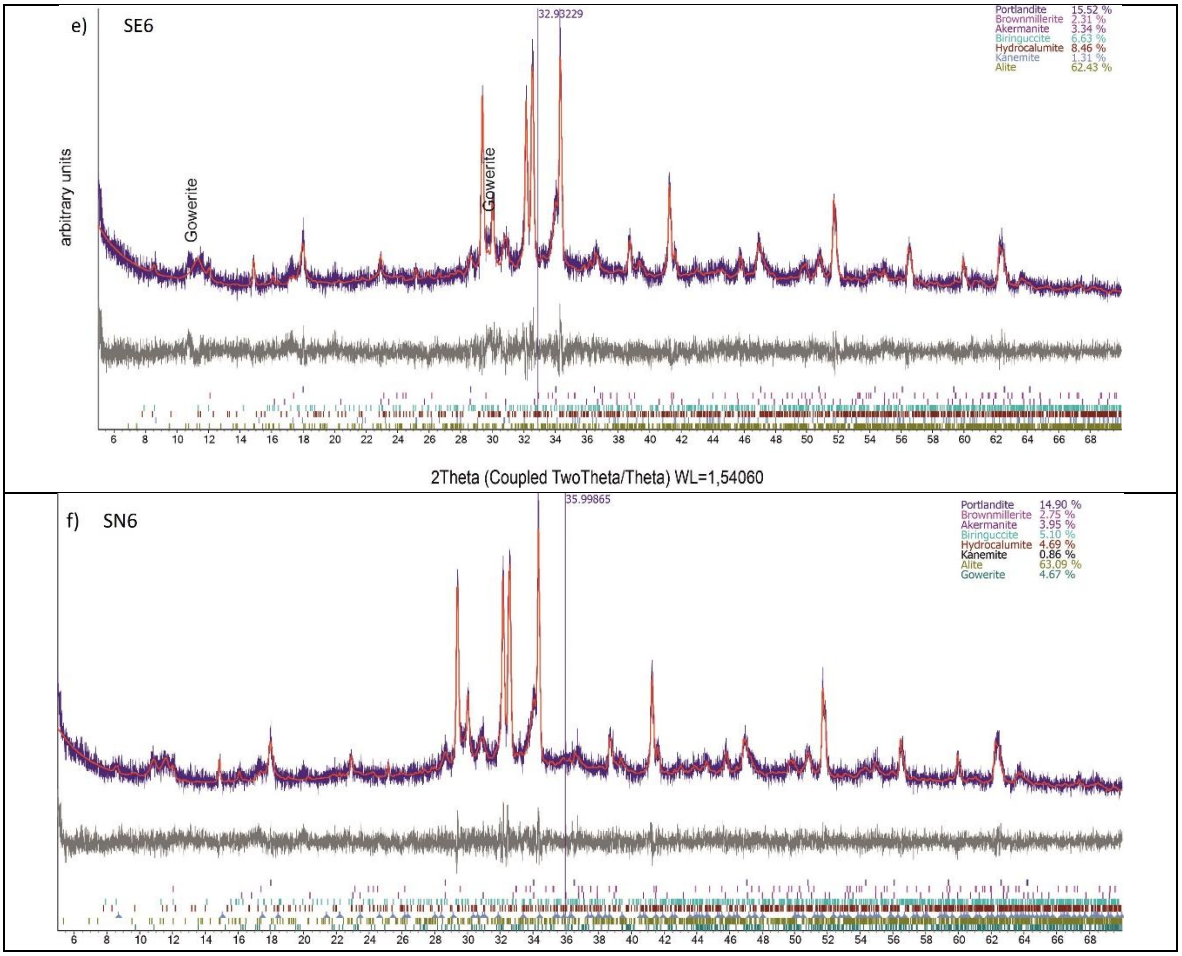

760 **Fig. S2** XRD patterns obtained before leached specimens.

761

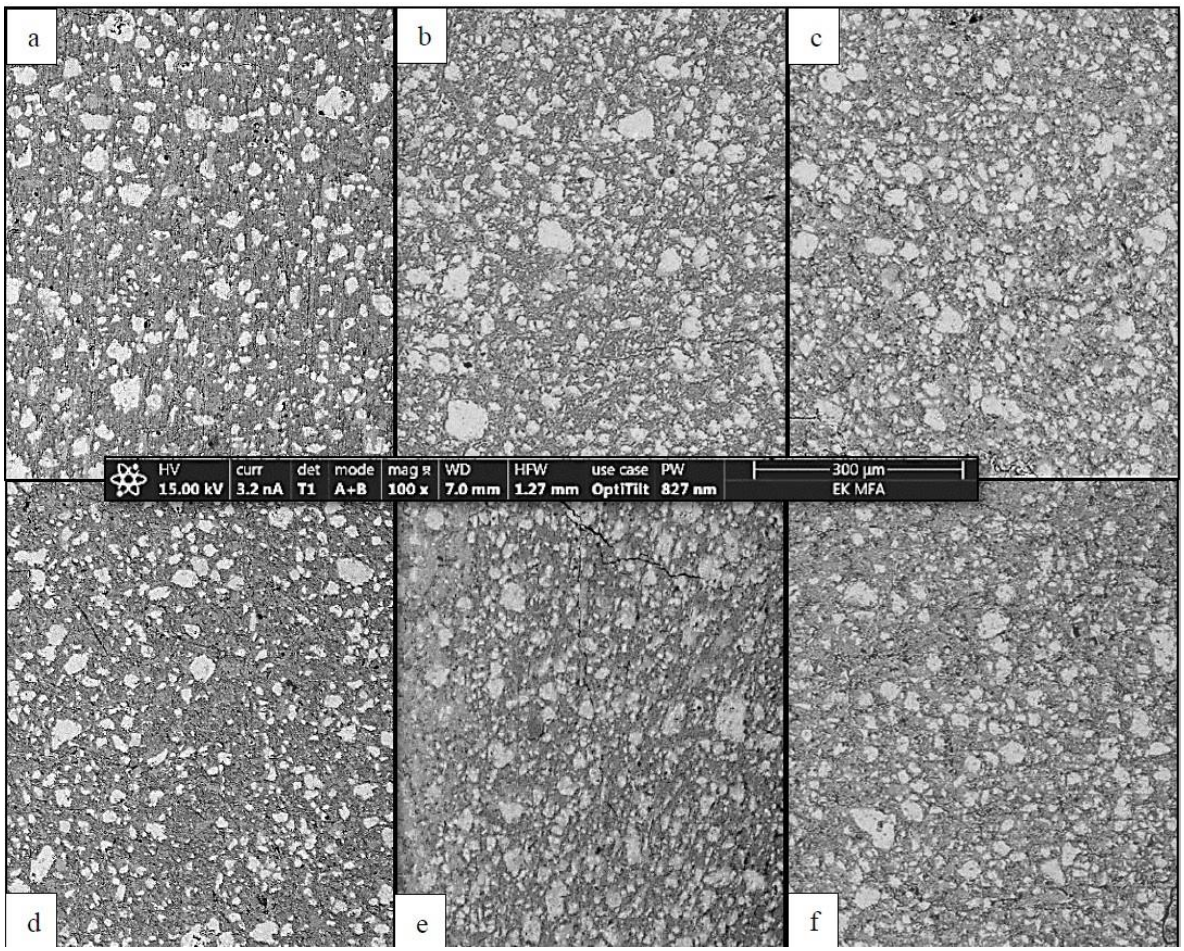

762

Fig. S3 Results of SEM analysis of the cementitious specimens before and after the leaching tests: a-c) BSE images of the samples before leaching made by NBA, containing 20, 40, and 60 g/l boron, respectively; d-f) BSE images of the samples before leaching made by EBA, containing 20, 40, and 60 g/l boron, respectively.

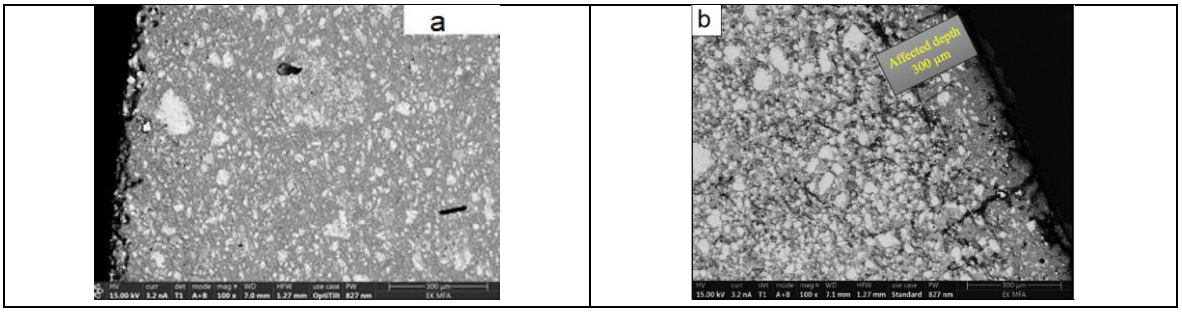

763

764 **Fig. S4.** Selected BSE image representative of the solidified waste forms showing before (a)
765 and after (b) leaching tests. The bright minerals represent the unreacted clinkers such as alite
766 and belite.

767

768

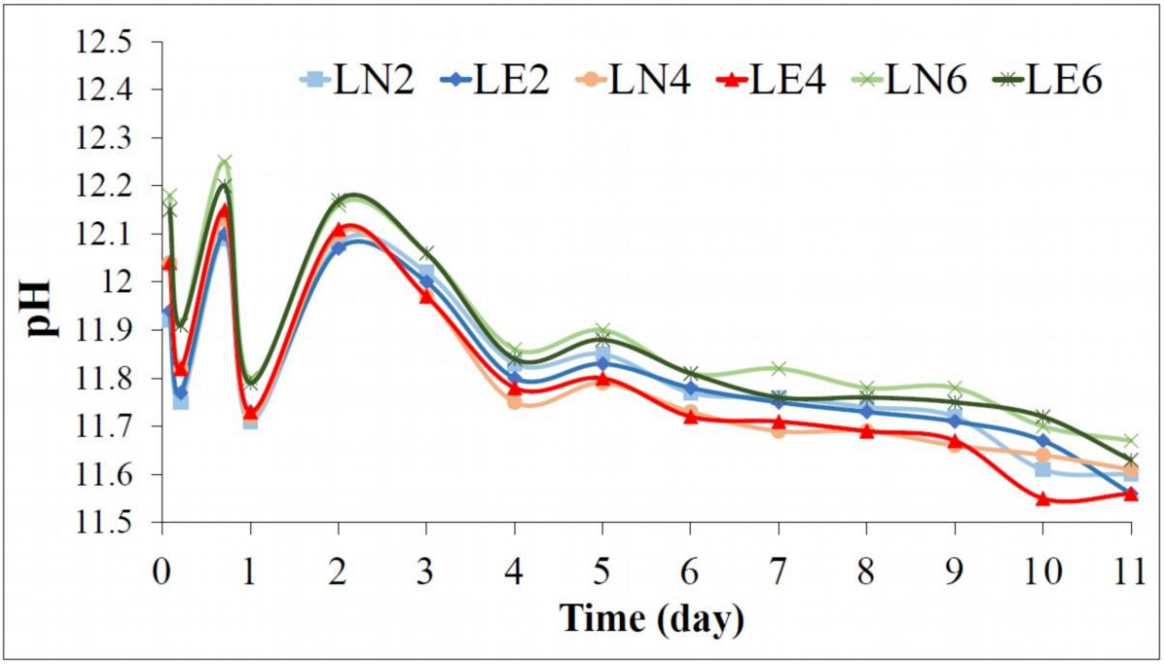

Fig. S5 pH value of the leachates vs. time during the leaching test

*LN: leachate from the solidified specimens containing natural boric acid (19.9% 10B); LE: leachate from the solidified specimens containing enriched boric acid (95% 10B); 2, 4, and 6 are representatives for 20, 40, and 60 g/l boron in the simulated liquid wastes